iScience

CellPress
OPEN ACCESS

Article

Stress-induced NEDDylation promotes cytosolic protein aggregation through HDAC6 in a p62-dependent manner

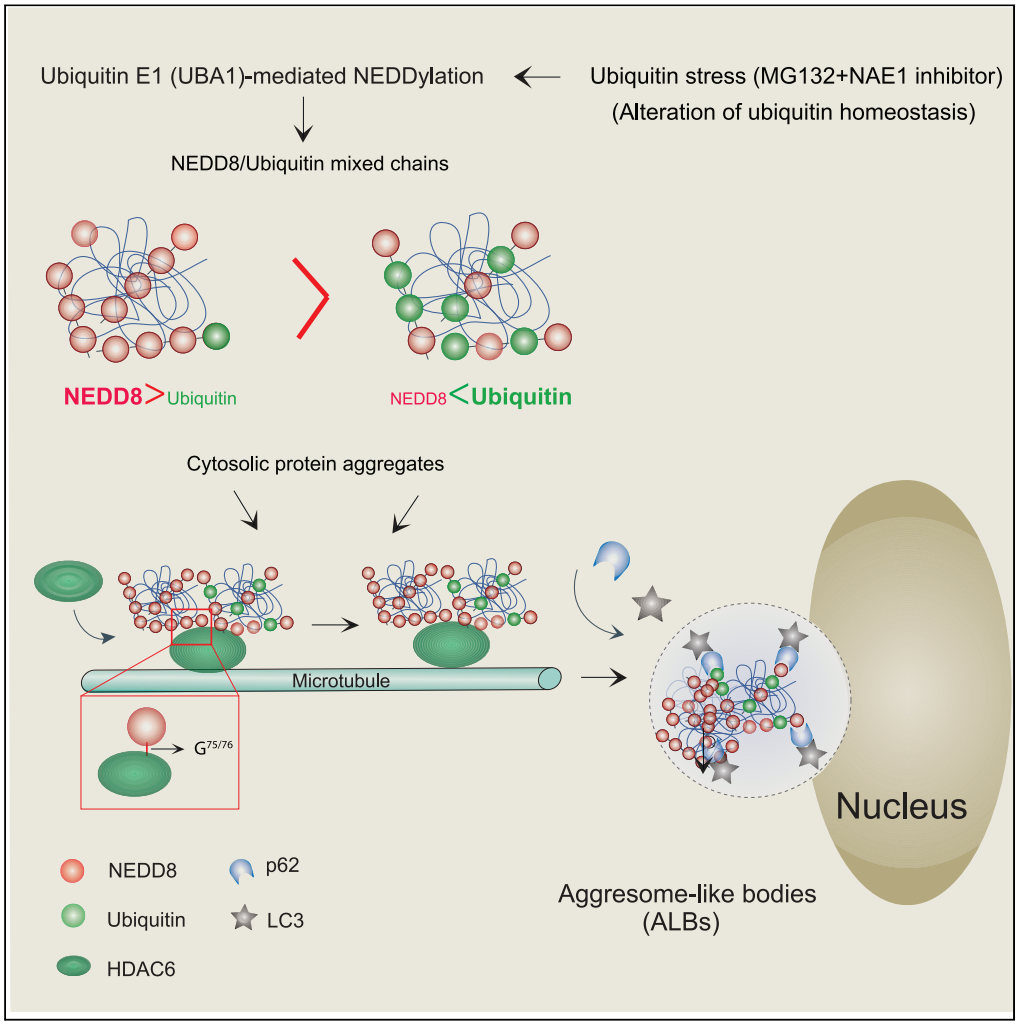

Soyeon Kim, Mira Kwon, Yiseul Hwang, Junghyun Yoon, Sangwook Park, Ho Chul Kang

hckang@ajou.ac.kr

HIGHLIGHTS

NEDD8 directly binds to HDAC6 and regulates the formation of aggresome-like body (ALB)

HDAC6 carries NEDDylated cytosolic protein aggregates into ALBs under ubiquitin stress

p62 directly controls ALBs formation as an acceptor of NEDDylated cytosolic aggregates

The NEDD8-HDAC6-p62 axis controls proteostasis by forming ALB-coupled autophagy

Kim et al., iScience *24*, 102146
March 19, 2021
https://doi.org/10.1016/j.isci.2021.102146

iScience

CellPress
OPEN ACCESS

Article

Stress-induced NEDDylation promotes cytosolic protein aggregation through HDAC6 in a p62-dependent manner

Soyeon Kim,[1,2] Mira Kwon,[1,2] Yiseul Hwang,[1,2] Junghyun Yoon,[1,2] Sangwook Park,[1,2] and Ho Chul Kang[1,2,3,*]

SUMMARY

Stress-coupled NEDDylation potentially regulates the aggregation of nuclear proteins, which could protect the nuclear ubiquitin-proteasome system from proteotoxic stress. However, it remains unclear how NEDDylation controls protein-aggregation responses to diverse stress conditions. Here, we identified HDAC6 as a direct NEDD8-binding partner that regulates the formation of aggresome-like bodies (ALBs) containing NEDDylated cytosolic protein aggregates during ubiquitin stress. HDAC6 colocalizes with stress-induced ALBs, and HDAC6 inhibition suppresses ALBs formation, but not stress-induced NEDDylation, suggesting that HDAC6 carries NEDDylated-proteins to generate ALBs. Then, we monitored the ALBs-associated proteostasis network and found that p62 directly controls ALBs formation as an acceptor of NEDDylated cytosolic aggregates. Interestingly, we also observed that ALBs are highly condensed in chloroquine-treated cells with impaired autophagic flux, indicating that ALBs rely on autophagy. Collectively, our data suggest that NEDD8, HDAC6, and p62 are involved in the management of proteotoxic stress by forming cytosolic ALBs coupled to the aggresome-autophagy flux.

INTRODUCTION

Quality control of cellular proteins is strictly regulated by either the ubiquitin proteasome system (UPS) and/or autophagy machinery (Dikic, 2017; Lilienbaum, 2013). The UPS is the main means of removing ubiquitinated proteins, and its dysfunction triggers the accumulation of abnormal misfolded proteins, which form aggregates that interfere with the normal cellular functions, ultimately leading to cellular stress and altered cell viability (Chen et al., 2011; Ciechanover and Kwon, 2015). Notably, up to 30% of the newly synthesized proteins within eukaryotic cells are misfolded (Schubert et al., 2000). Thus, efficient management of misfolded proteins is critical to the maintenance of proteostasis and cell survival. Cells have evolved several organized pathways to regulate misfolded protein-derived cytotoxic aggregates, which are a hallmark of various neurodegenerative diseases, including Alzheimer and Parkinson diseases (Dong and Cui, 2018; Hipp et al., 2019; Taylor et al., 2002). However, whether transient or chronic protein aggregation causes UPS toxicity or whether the UPS is a part of the defense mechanism against protein toxicity remains debatable (Bence et al., 2001; Bennett et al., 2005; Deriziotis et al., 2011; Kim et al., 2016; Lindersson et al., 2004; Lorenzo and Yankner, 1996; Schipper-Krom et al., 2012; Treusch et al., 2009).

Ubiquitin and the E3 ligases, involved in the UPS and autophagy, interpret and translate proteotoxic signals into appropriate cellular responses without compromising cellular integrity (Ciechanover et al., 2000; Hershko and Ciechanover, 1998; Kocaturk and Gozuacik, 2018; Komander and Rape, 2012). Indeed, dysregulated activity of the ubiquitin-dependent protein degradation system is implicated in several age-related diseases in humans (Limanaqi et al., 2020; Ross and Poirier, 2004; Vilchez et al., 2014). Mutations, aging, and environmental stress lead to dramatically reduced proteasomal activity and result in the production of misfolded proteins (Saez and Vilchez, 2014; Vilchez et al., 2014). These proteins are captured by specific ubiquitin E3 ligases and become polyubiquitinated, resulting in the accumulation of ubiquitinated protein aggregates that cause an imbalance in the ubiquitin pool, leading to ubiquitin stress (Amm et al., 2014; Chhangani et al., 2013; Dantuma and Lindsten, 2010; Peng et al., 2017). UPS impairment

[1]Department of Physiology, Ajou University School of Medicine, World cup-ro, Yeongtong-gu, Suwon, Gyeonggi 16499, Republic of Korea

[2]Department of Biomedical Sciences, Graduate School of Ajou University, World cup-ro, Yeongtong-gu, Suwon, Gyeonggi 16499, Republic of Korea

[3]Lead contact

*Correspondence: hckang@ajou.ac.kr

https://doi.org/10.1016/j.isci.2021.102146

enhances compensatory autophagy, which is an attempt made by the cell to remove or sequester cytotoxic ubiquitinated protein aggregates and maintain proteostasis. However, the molecular networks underlying this compensation are poorly characterized (Chen et al., 2011; Peng et al., 2017; Wang and Wang, 2015).

NEDD8 is a protein that has 60% sequence identity and 80% homology to ubiquitin (Kamitani et al., 1997; Whitby et al., 1998) and has been proposed as a new modifier that promotes nuclear protein aggregation and protects the nuclear UPS through atypical NEDDylation, which requires ubiquitin-activating enzyme E1 (UBA1) rather than NEDD8 E1-activating enzyme (NAE1) as shown in an UPS impairment model (Maghames et al., 2018). Although the functional roles of NEDD8 in cellular proteostasis were established primarily through the regulation of Cullin-RING-ligases (Petroski and Deshaies, 2005), more recent studies show that the UBA1-coupled NEDDylation pathway induces atypical NEDDylation in response to various cellular stresses, including proteasomal impairment, heat shock, and oxidative stress (Leidecker et al., 2012; Li et al., 2015). In general, NEDDylation requires the NAE1 enzyme, which is a heterodimer of APPBP1 and UBA3, to activate NEDD8 (Gong and Yeh, 1999). However, UBA1, not NAE1, can activate NEDD8 during atypical NEDDylation under ubiquitin stress, wherein the level of endogenous NEDD8 is higher than that in the ubiquitin pool (Hjerpe et al., 2012a). This is also supported by the previous observation that exogenously overexpressed NEDD8 induces atypical NEDDylation via the activation of the ubiquitination pathway (Hjerpe et al., 2012b). Indeed, changes in the cellular ubiquitin pool that have been linked to ubiquitin stress are critically associated with numerous biological or pathophysiological conditions, such as heat shock, aging, and neurodegenerative diseases (Grabbe et al., 2011; Hanna et al., 2007; Lee et al., 2016). Interestingly, accumulation of NEDD8 in ubiquitinated inclusions was detected in the brains of patients diagnosed with neurodegenerative diseases that are linked to UPS dysfunction (Dil Kuazi et al., 2003; Mori et al., 2005), suggesting that NEDDylation-mediated protein aggregation is associated with the pathophysiology of the disease. Although the aforementioned studies suggest a link between NEDD8 and UPS dysfunction, the biological significance of the UBA1-dependent NEDDylation in response to ubiquitin stress remains unclear. In addition, the identity of the cellular proteins that are involved in atypical NEDDylation-mediated protein aggregation and whether this phenomenon is a common stress response at the cellular level remains unclear.

In this study, we identified histone deacetylase 6 (HDAC6) as a carrier of stress-induced NEDDylated proteins that facilitate the formation of transient protein aggregates in the cytoplasm rather than nucleus, thereby leading to the formation of aggresome-like bodies (ALBs) during ubiquitin stress. Furthermore, we observed that p62 acts as an acceptor for NEDDylated aggregates to promote ALB formation. Based on the results of this study, we propose that ubiquitin stress promotes NEDDylation-dependent cytoplasmic protein aggregation and that transiently formed protein aggregates interact with the molecular machinery of the aggresome-autophagy flux to control proteotoxic stress.

RESULTS

Identification of HDAC6 as a NEDD8-binding protein

Although stress-induced NEDDylation might be associated with various signaling pathways that underlie several pathophysiological states, little is known about its function (in comparison to ubiquitination). Therefore, identifying binding partners of NEDD8 may provide a link between NEDDylation and downstream signaling pathways that contribute to the pathogenesis of different diseases. To address this, we utilized the HuProt v3.0 human proteome microarray (CDI Laboratories, USA), which contain over 21,000 human proteins, to identify proteins that bind directly to NEDD8. We identified 17 proteins as directly interacting partners of NEDD8, which show a signal-to-noise ratio (SNR) > 1.0 (Figures 1A and S1A). To validate our protein microarray results, 16 proteins (not including NEDD8) were monitored for their ability to bind to NEDD8 using an immunoprecipitation assay. We found that 13 proteins were capable of binding to NEDD8, indicating that 81.2% of the results obtained using the human protein microarray were true positives (Figure S1B). Among these 13 proteins, we selected HDAC6, a histone deacetylase and ubiquitin-binding receptor for aggresome formation (Lee et al., 2010; Ouyang et al., 2012), and characterized its NEDD8-linked functions. Coexpression analysis clearly showed that HDAC6 colocalized with NEDD8 in the cytoplasm, as evidenced by a speckled staining pattern in the presence of MG132, which is a proteasome inhibitor (Figure 1B). In agreement with the protein microarray data, dot-blot and octet-based binding analysis showed that HDAC6 bound directly to NEDD8 with high affinity (KD = 1.18 nM; Figures 1C and 1D). Collectively, these results suggest that NEDD8 directly binds to

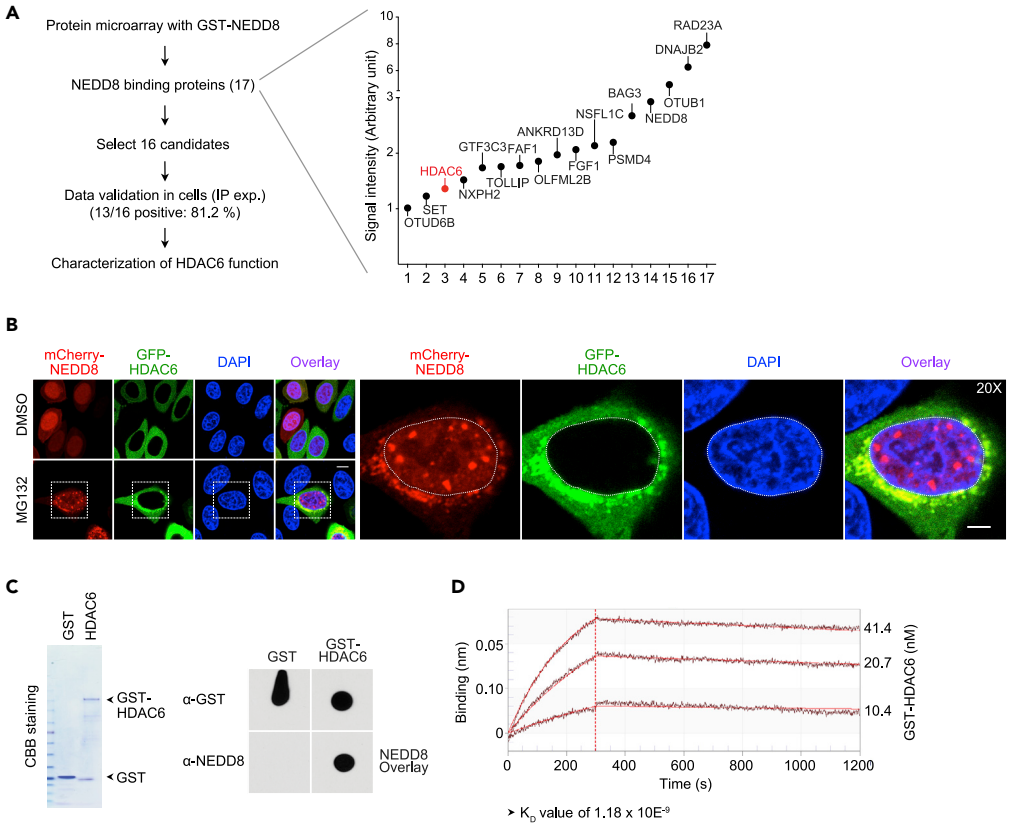

Figure 1. Identification of HDAC6 as a novel NEDD8-binding partner

(A) Schematic illustration of strategy for profiling the NEDD8-binding proteins using a protein microarray (left panel). Total 17 proteins containing NEDD8 were identified as a NEDD8 binding proteins (right panel).

(B) HeLa cells were transfected with mCherry-NEDD8 and GFP-HDAC6, and the colocalization of two proteins was analyzed in the absence or presence of MG132 (5 μM). Enlarge insets represent the NEDD8/HDAC6-colocalized structure observed in perinuclear region upon MG132 treatment. Nuclei were stained with DAPI (blue). DMSO was used as a negative control.

(C) Recombinant GST and GST-HDAC6 were loaded in 8%–16% SDS-PAGE and visualized by staining with Coomassie Brilliant Blue (left panel). Dot blot assay was performed with recombinant NEDD8 and HDAC6 as indicated. NEDD8-binding activity to HDAC6 was detected by anti-NEDD8 antibody (right panel). GST was used as a negative control.

(D) The kinetic interaction of NEDD8 to HDAC6 was monitored at pH 4.0 using the Octet QKe System (ForteBio) as describe in Transparent Methods.

See also Figure S1.

HDAC6 with a high affinity and forms speckled cytoplasmic structures in lysosome- and proteasome-enriched perinuclear regions.

NEDD8 binds to HDAC6 via a C-terminal di-glycine (di-Gly) motif

The zinc-finger ubiquitin-binding domain (ZnF-UBP) of HDAC6 forms a deep pocket that specifically binds to the C-terminal di-Gly residues (G75-G76) of unanchored ubiquitin (Ouyang et al., 2012). In a manner similar to ubiquitin, NEDD8 precursors contain di-Gly residues with a pentapeptide extension (GGLRQ) at the C-terminal that is cleaved, resulting in a C-terminal di-Gly motif in the mature protein (Wada et al., 1998). Thus, NEDD8 can access the HDAC6-binding site in a similar fashion to that of ubiquitin. To monitor whether the C-terminal glycine residues of NEDD8 are required for interaction with HDAC6, we generated three different C-terminal glycine mutants including GST- or V5-tagged NEDD8 WT, NEDD8^{G75A,G76A} ($G^{75/76}A$ mutant), NEDD8^{G77A,G78A} ($G^{77/78}A$ mutant), and NEDD8$^{G75\sim G78A}$ ($G^{75\sim78}A$ mutant), and purified them from insect cells. GST-tagged NEDD8 proteins were purified from insect cells, and the GST-tag was then removed from the purified proteins by enzymatic cleavage. The purity of GST-free NEDD8 proteins was estimated by Coomassie

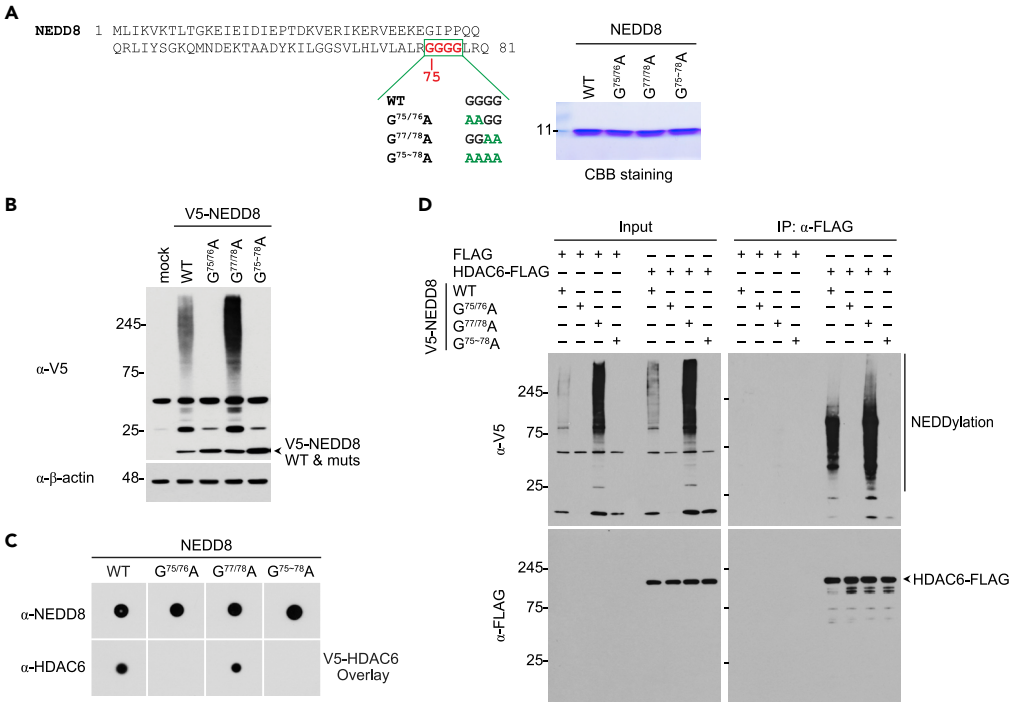

Figure 2. NEDD8 interacts with HDAC6 *via* di-glycine motif on its c-terminal

(A) Schematic illustration of protein sequences for NEDD8 WT and mutants (left panel). NEDD8 WT and its mutant proteins were purified from insect Sf9 cells, and the purity of each protein was checked by 8%–16% SDS-PAGE as indicated (right panel).

(B) V5-tagged NEDD8 WT and its mutants were transfected into U2OS cells and then their ability for NEDD8 conjugation was monitored by immunoblotting with anti-HRP-conjugated V5 antibody.

(C) Dot blot assay was performed with recombinant NEDD8, its mutants, and HDAC6 as indicated.

(D) HDAC6-FLAG was transfected into HEK293FT along with V5-tagged NEDD8 WT or its mutants. After 48 h, cells were harvested and lysed, and then HDAC6-FLAG were immunoprecipitated using anti-FLAG M2 agarose. Samples were separated by 8%–16% SDS-PAGE and analyzed by immunoblotting with anti-HRP-conjugated V5 and anti-HRP-conjugated FLAG antibodies.

staining after sodium dodecyl-polyacrylamide gel electrophoresis (SDS-PAGE) of the total protein (Figure 2A). Next, we assessed the levels of NEDDylation in U2OS cells transfected with V5-tagged NEDD8 plasmids. As expected, expression analysis revealed that—as in case of ubiquitin binding—the $G^{75/76}$ di-Gly residues of NEDD8 are required for the NEDDylation of cellular substrates (Figure 2B). In addition, *in vitro* dot-blot assays revealed that $G^{75/76}$ di-Gly residues of NEDD8 are also essential for interaction with HDAC6 (Figure 2C). Consistent with *in vitro* data, co-expression analysis showed that substrates NEDDylated with WT NEDD8 and the $G^{77/78}$A mutant strongly bind to HDAC6, whereas the $G^{75/76}$A and $G^{75\sim78}$A mutants failed to interact with HDAC6 in cells, suggesting that HDAC6 may be involved in NEDD8 metabolism in a similar way to that of ubiquitin (Figure 2D).

HDAC6 colocalizes with NEDDylated cytosolic aggregates in ALBs

Next, to address the physiological relevance of HDAC6 and NEDD8, we evaluated their endogenous subcellular distribution in the presence or absence of MG132. Unexpectedly, endogenous NEDD8 does not colocalize with endogenous HDAC6, even when treated with MG132 (Figure 3A). This result raised the question as to which physiological conditions induce the interaction between NEDD8 and HDAC6. As shown in Figure 1B, ectopically expressed NEDD8 forms cytosolic aggregates with HDAC6 in the perinuclear region. Therefore, we hypothesized that the accumulation NEDD8 protein and/or NEDD8-conjugated proteins may affect the generation of cytosolic aggregates. Recently, it was reported that the balance between protein modification by ubiquitin or NEDD8 is dramatically regulated by cellular stress, which alters ubiquitin homeostasis, and this phenomenon is termed as "ubiquitin stress" (Kimura and Tanaka, 2010; Leidecker et al., 2012; Park and Ryu, 2014). Thus, the physiological interaction between

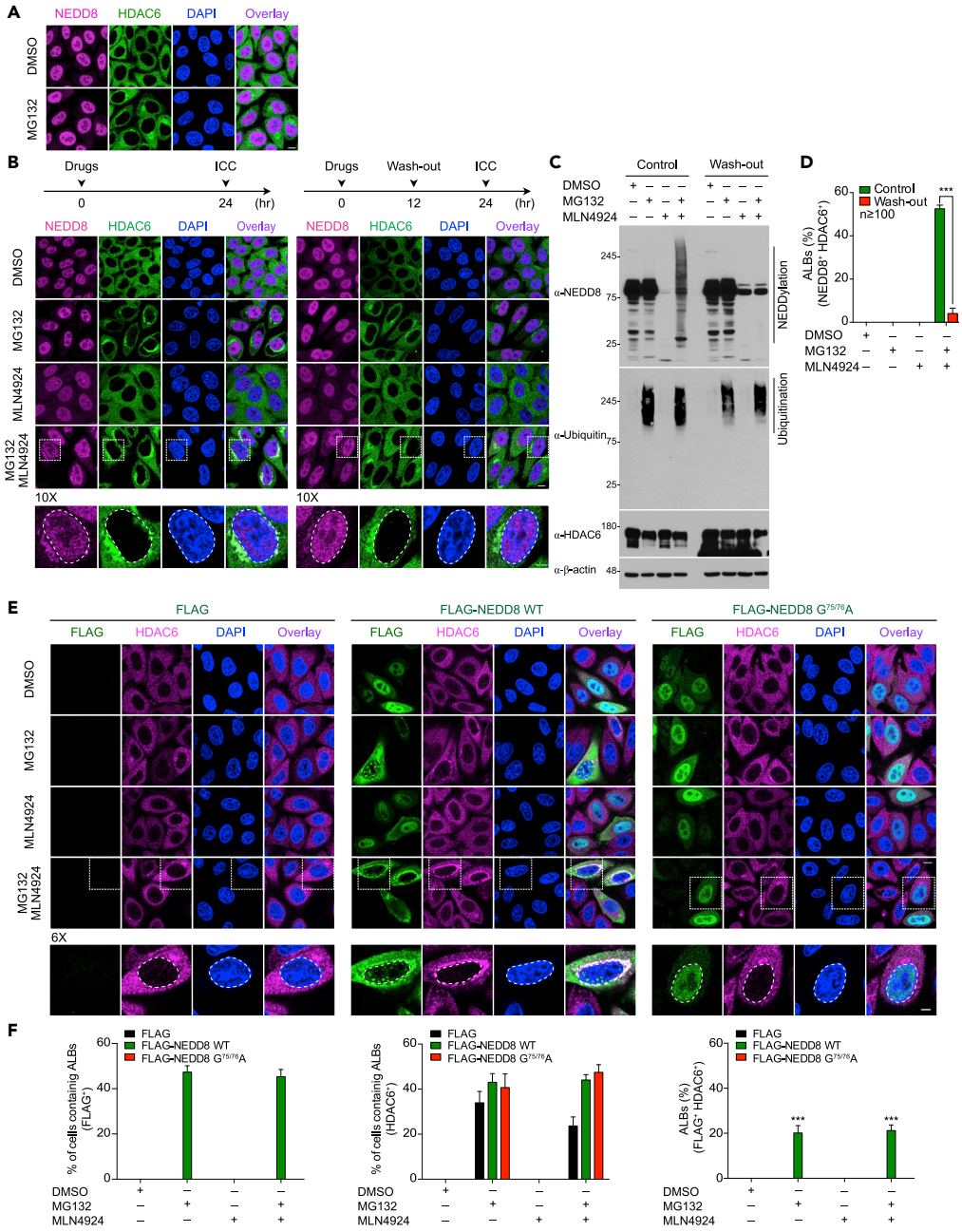

Figure 3. HDAC6 localizes in aggresome-like bodies (ALBs) with NEDDylated cytosolic aggregates

(A) HeLa cells were treated DMSO or 5 μM MG132 for 12 h. Endogenous NEDD8 (pink) and HDAC6 (green) were visualized by immunostaining with anti-NEDD8 and anti-HDAC6 antibodies, respectively.

(B–D) HeLa cells were treated with DMSO, MLN4924 (3 μM), MG132 (5 μM) as single or in combination as indicated. For the washout experiment, cells treated with each reagent for 12 h were washed twice in PBS, followed by culture with normal media for 12 h (right panel). After 24 h, cells were immunostained with anti-NEDD8 and anti-HDAC6 antibodies. Scale bars, 10 μm. Enlarge insets represent the NEDD8/HDAC6-colocalized ALBs structure observed in perinuclear region upon MG/MLN treatment. White square boxes show the location of the magnified region. Scale bars, 5 μm (B). Experiment was performed as above and cell lysates were subjected into immunoblot analysis as indicated (C). The quantification of cells containing ALBs in B (D).

(E and F) Similar experiments as in B with the exception that FLAG, FLAG-NEDD8 WT, or FLAG-NEDD8 $G^{75/76}A$ were transfected. Endogenous HDAC6 (pink) or FLAG (green) was visualized by immunostaining as indicated (E). Scale bars, 10 μm. The quantification of cells containing ALBs in E (F). Enlarge insets represent the FLAG, FLAG-NEDD8 WT, or

Figure 3. *Continued*
FLAG-NEDD8 $G^{75/76}A$/HDAC6-colocalized structure observed in MG/MLN-treated cells. Scale bars, 5 μm. Nuclei were counterstained with DAPI. "+" denotes positive cells showing ALBs formation with indicated markers. Data represent mean ± SEM of three independent experiments. ***$p \leq 0.01$.
See also Figure S2.

HDAC6 and NEDD8 might be affected by the cellular balance between ubiquitin and NEDD8 during ubiquitin stress. To test this hypothesis, we assessed the localization of NEDD8 and HDAC6 after administration of MG132 and the NEDD8-activating enzyme E1 subunit 1 (NAE1) inhibitor MLN4924, which induce robust NEDDylation following the induction of ubiquitin stress (Leidecker et al., 2012). Remarkably, we found that when MG132 and MLN4924 (hereafter MG/MLN) were simultaneously administered, NEDD8 and HDAC6 colocalized in the perinuclear region (Figure 3B). Upon co-staining endogenous proteins, we also observed that NEDD8 and HDAC6 formed cytosolic aggregates, culminating in ALBs formation around the nuclear membrane (Figure 3B). Intriguingly, as shown Figure 1B, ALBs were also observed in NEDD8 overexpressing cells treated with MG132. These data suggest that ALBs formation is induced by alterations in NEDD8 levels and the induction of ubiquitin stress in which NEDD8 interacts with HDAC6 to produce cytosolic protein aggregates. Indeed, immunoblotting shows that only MG/MLN-induced ubiquitin stress results in robust NEDDylation and ALBs formation, suggesting that HDAC6 may regulate NEDDylation-mediated ALBs formation during ubiquitin stress (Figure 3C). In addition, ALBs generated in response to ubiquitin stress reduced when MG/MLN was removed from the culture media, resulting in an approximate 90% reduction in ALBs formation (Figure 3D). These results suggest that ubiquitin stress-induced NEDDylation and accompanying ALB formation may be a reversible process that transiently occurs in the cytoplasm via the interaction between NEDD8 and HADC6. However, it is still unclear whether NEDD8 directly controls ALBs formation by direct interaction with HDAC6 under ubiquitin stress. Thus, to elucidate this, we monitored MG/MLN-induced ALB formation in response to overexpression of FLAG-NEDD8 $G^{75/76}A$ that does not bind to HDAC6 and cannot induce NEDDylation. Overexpression analysis clearly showed that endogenous HDAC6 colocalized with ectopically overexpressed FLAG-NEDD8 WT in the perinuclear region to form ALBs. However, we found that FLAG-NEDD8 $G^{75/76}A$ failed to interact with endogenous HDAC6, suggesting that ALBs formation is not only induced by direct interaction between HDAC6 and NEDD8 via the di-Gly motif but also requires ubiquitin stress-induced NEDDylation (Figures 3E and 3F). To further validate this result, we tested the effect of a NEDD8 knockdown on ALBs formation under the same ubiquitin stress conditions. As expected, we observed that NEDD8 knockdown dramatically leads to a reduction in ubiquitin stress-induced NEDDylation and results in a 100% reduction in ALBs formation (Figures S2A and S2B). Transfection with control siRNA did not result in any significant changes, suggesting that NEDD8 is directly involved in the regulation of ubiquitin stress-induced ALBs formation with HDAC6. The knockdown efficiency was evaluated by an immunoblot assay using a NEDD8 antibody (Figure S2C). In parallel, we also estimated the impact of a knockdown of endogenous ubiquitin because it can also alter ubiquitin homeostasis in a manner similar to NEDD8 knockdown. Consistent with the previous results, we found that stress-induced NEDDylation was strongly induced upon ubiquitin knockdown (Figure S2D). Unexpectedly, however, we observed that ubiquitin depletion caused nuclear aggregation of NEDD8, whereas control siRNA-treated cells showed cytosolic aggregation of NEDD8 (Figure S2D). This is similar to previous reports that suggest that NEDDylation induced by heat stress promotes nuclear aggregation of proteins (Maghames et al., 2018), wherein they estimated the nuclear accumulation of NEDDylated aggregates at the nucleolus in response to acute inhibition of proteasomes with high-dose MG132. These results suggest that the induction and accumulation of NEDDylation can be differently regulated based on the type of stimulus. To assess this, additional experimental conditions of shorter treatment times of 2 or 5 h with high-dose MG132 (25 μM) were used. As shown in the Figure S2F, NEDDylation was slightly enhanced upon treatment with high concentrations of MG132, but the increase was not very large compared with that of cells treated with MG/MLN for 12 h (Figure S2F). This is quite interesting because it suggests that both stimuli can induce alterations in ubiquitin homeostasis, but NEDDylation may be differently regulated based on the stimulus type. Nonetheless, we focused on NEDDylation-mediated cytosolic protein aggregation, as cytosolic inclusions of NEDD8 are primarily detected in various age-related diseases (Dil Kuazi et al., 2003; Mori et al., 2005).

UBA1-dependent NEDDylation is crucial for ALB formation

Previously, it has been reported that ubiquitin stress strongly induces atypical NEDDylation in a UBA1-dependent and a NAE1-independent manner (Leidecker et al., 2012). Thus, to examine the role of UBA1 in the regulation of ALBs formation during ubiquitin stress, we estimated the relative percentage of cells

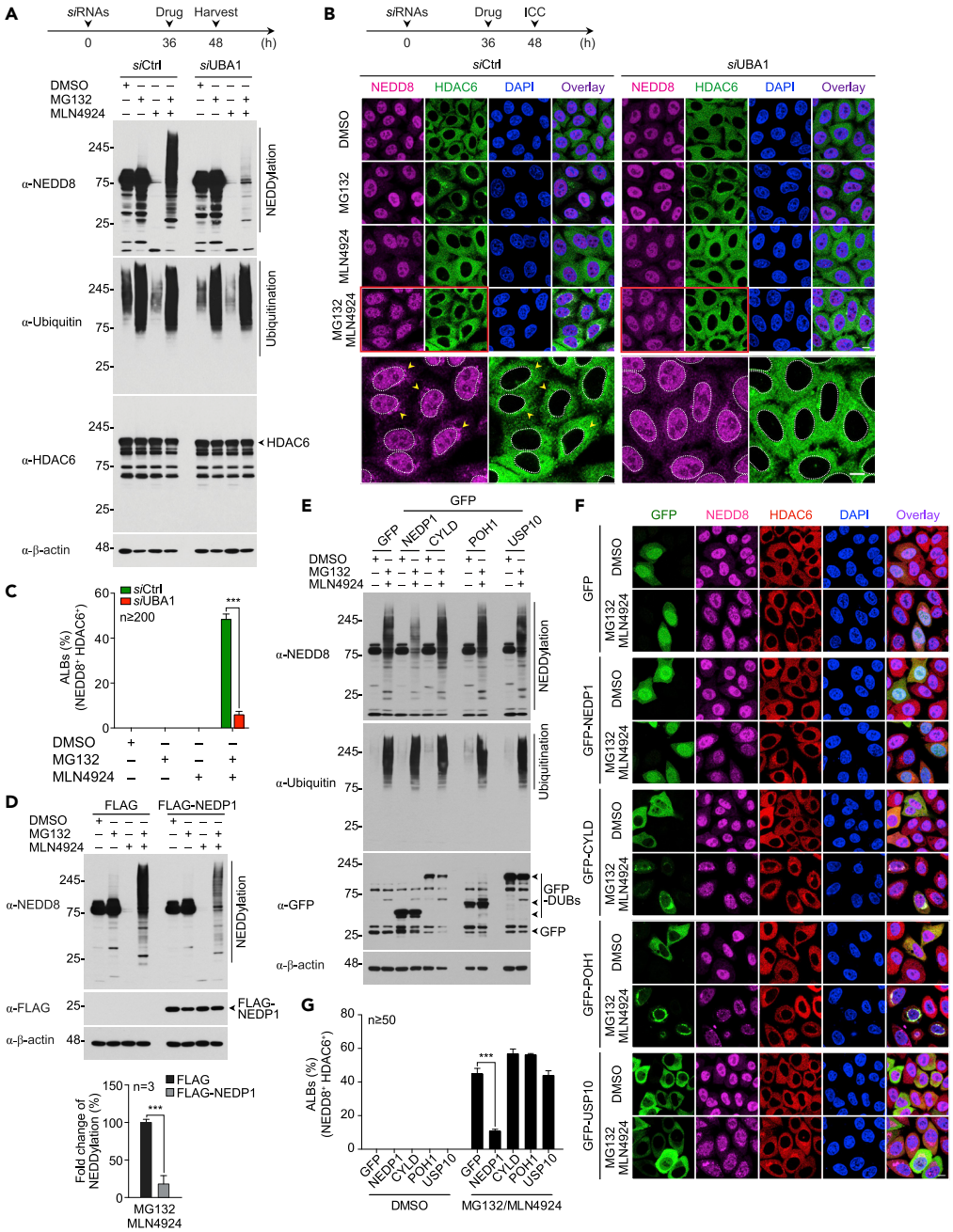

Figure 4. NEDDylation-mediated ALBs formation is mainly controlled by UBA1 with NEDD8 rather than ubiquitin

(A–C) HeLa cells were transfected with *si*Ctrl or *si*UBA1 in the absence/presence of indicated reagents for 12 h. After 48 h, whole-cell lysates were prepared and loaded by 8%–16% SDS-PAGE. Immunoblotting analysis was performed with indicated antibodies (A). Experiment was performed as above, and cells were stained with anti-NEDD8 and anti-HDAC6 antibodies. Enlarge insets represent the NEDD8/HDAC6-colocalized structure observed in MG/MLN-treated cells. Arrowheads indicate ALBs. Scale bars, 10 μm (B). The cells containing ALBs were quantified and represented as graph as indicated (C).

(D–G) HeLa cells were transfected with FLAG or FLAG-NEDP1 and then treated with reagents as indicated. After 48 h, cells were lysed and then cell lysates were subjected into immunoblotting assay with indicated antibodies (upper panel). The level of NEDDylation was quantified by ImageJ software (lower panel) (D). Indicated plasmids were transfected into HeLa cells and then treated with either DMSO or MG/MLN. The level of NEDDylation was monitored as indicated (E). Experiment was performed as above, and cells were stained with anti-NEDD8 and anti-HDAC6 antibodies (F). The cells containing ALBs were quantified as described in C (G).

Figure 4. *Continued*
Nuclei were counterstained with DAPI. "+" denotes positive cells showing ALBs formation with indicated markers. Data represent mean ± SEM of three independent experiments. ***$p \leq 0.01$.
See also Figures S3 and S4.

containing ALBs after UBA1 depletion (Figures 4A, 4B, and S3A). We observed that UBA1 knockdown affects ubiquitin stress-induced NEDDylation (Figure 4A) and results in a 95% reduction in ALBs formation (Figures 4B and 4C). Transfection with control siRNA did not result in any significant changes, suggesting that UBA1 is essential for ubiquitin stress-induced ALB formation via NEDDylation. Furthermore, we found that the NEDD8 E2 enzymes, UBE2F and UBE2M, that are involved in canonical NEDDylation are not required for UBA1-dependent NEDDylation (Figure S3B). These results suggest that although UBA1 is indispensable for ALBs formation, canonical NEDDylation machinery is not required for this process.

Next, we examined whether NEDD8 chains on NEDDylated substrates are specifically required for ALBs formation. Cell lysates were treated with recombinant NEDP1, a NEDD8-specific deNEDDylase (Wu et al., 2003). As expected, NEDP1 removed NEDD8 chains from NEDDylated substrates produced in response to ubiquitin stress, but there was no effect on ubiquitination signaling (Figure S4A). Consistent with *in vitro* data, ectopically expressed NEDP1 resulted in a 70% reduction of NEDDylation in cells (Figure 4D). UBA1-dependent NEDDylation is mainly achieved by the formation of hybrid NEDD8/ubiquitin conjugates with substrates (Leidecker et al., 2012; Maghames et al., 2018). To elucidate whether hybrid NEDD8/ubiquitin chains are involved in ubiquitin stress-induced NEDDylation and whether these chains are required for ALBs formation, cells were transfected with GFP-tagged NEDP1 or ubiquitin-specific deubiquitylases (DUBs), namely CYLD, POH1, and USP10, which are aggresome- or proteasome-associated DUBs (Hao et al., 2013; Takahashi et al., 2018; Wickstrom et al., 2010), in the absence or presence of MG/MLN (Figures 4E, 4F, and 4G). Surprisingly, ubiquitin stress-induced NEDDylation was decreased upon ectopic expression of NEDP1; however, other DUBs did not induce a significant reduction in NEDDylation (Figure 4E). To exclude the possibility that DUBs have no protease activity against ubiquitin chains in the aforementioned experiment, we performed an additional experiment to show the protease activity of CYLD with recombinant ubiquitin chains, branched at K48 or K63, or MG/MLN-treated cell lysates in a similar way to that shown in Figure 4E. Expectedly, we observed that recombinant CYLD showed high enzymatic activity against K63-linked rather than K48-linked ubiquitin chains (Figure S4B). Nonetheless, it was also observed that CYLD did not show any significant effect on deNEDDylation from cell lysates treated with MG/MLN, whereas NEDP1 strongly induces deNEDDylation (Figure S4C). To further validate whether MG/MLN induces NEDDylation composing of NEDD8/ubiquitin hybrid chains, we isolated the NEDD8 conjugates from MG/MLN-treated cell lysates using anti-NEDD8 antibody. In consistent with previous result, we found that isolated NEDD8 conjugates were deNEDDylated by incubation with NEDP1 and not CYLD (Figure S4D). These results strongly suggest that this NEDDylation is mainly achieved by NEDD8 and not ubiquitin, although we cannot exclude the possibility that ubiquitin is still required for the initiation or chain extension of UBA1-dependent NEDDylation, as described in other studies (Maghames et al., 2018). In parallel, we observed that the percentage of ubiquitin stress-mediated ALBs formation was dramatically decreased upon NEDP1 overexpression (Figures 4F and 4G). Surprisingly, we observed that all DUBs strongly colocalized with ubiquitin and HDAC6 in the presence of MG/MLN (Figure S4E). Notably, even if NEDP1 was highly expressed in MG/MLN-treated cells, HDAC6 still colocalized with ubiquitin without ALBs formation (Figure S4E), indicating that HDAC6 may play distinct roles in NEDDylation and ubiquitination in stress-induced conditions. These results strongly indicate that UBA1-mediated NEDDylation is a crucial step in ALBs formation and that this process requires NEDD8 rather than ubiquitin.

HDAC6 modulates ALB formation through deacetylation activity during ubiquitin stress

HDAC6 is a microtubule-associated deacetylase and is involved in the regulation of ubiquitin-dependent aggresome formation. In addition, HDAC6 can bind to both polyubiquitinated misfolded proteins and dynein motors, thereby promoting aggresome assembly (Kawaguchi et al., 2003). Thus, we hypothesized that ALBs formation may also be regulated by HDAC6 activity. To address this, we attempted to inhibit HDAC6 activity with tubacin, a specific HDAC6 inhibitor, in MG/MLN-treated cells (Figure 5A, left panel). Interestingly, we found that ubiquitin stress-induced ALBs formation is remarkably reduced by tubacin (~95%) (Figure 5A, right panel). More interestingly, a significant increase in NEDDylation level was also

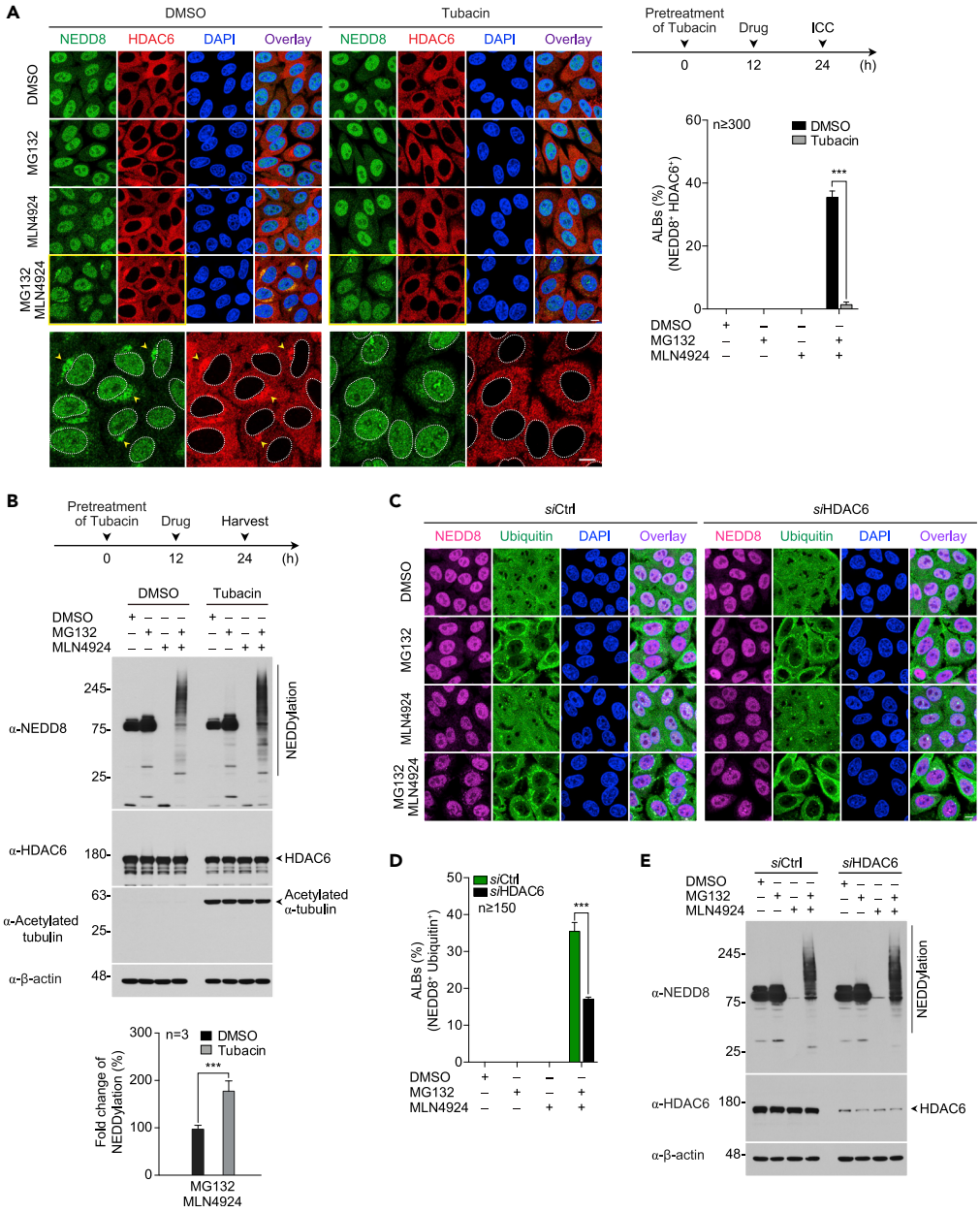

Figure 5. Deacetylase activity of HDAC6 is required for ALBs formation

(A) HeLa cells were pre-treated with 10 μM tubacin and followed by treatment with each reagent at indicated time points. Enlarge insets represent the NEDD8/HDAC6-colocalized structure induced by MG132/MLN4924 treatment in the absence/presence of tubacin (left panel). The cells containing ALBs were quantified as indicated (right panel). Scale bars, 10 μm.

(B) Experiment was performed as above, and cell lysates were immunoblotted with antibodies for NEDD8, HDAC6, acetylated α-tubulin, or β-actin, as indicated (upper panel). The level of NEDDylation was then quantified (lower panel).

(C–E) HeLa cells were transfected with *si*Ctrl or *si*HDAC6 and then treated with indicated reagents for 12 h. After 48 h, cells were stained with anti-NEDD8 and anti-ubiquitin antibodies (C), and the cells containing ALBs were quantified (D). Experiment was performed as above, and whole-cell lysates were prepared and loaded by 8%–16% SDS-PAGE. Immunoblotting analysis was performed with indicated antibodies. Arrowheads indicate ALBs. Scale bars, 10 μm (E). Nuclei were counterstained with DAPI. "+" denotes positive cells showing ALBs formation with indicated markers. Data represent mean ± SEM of three independent experiments. ***$p \leq 0.01$. Nuclei were counterstained with DAPI.

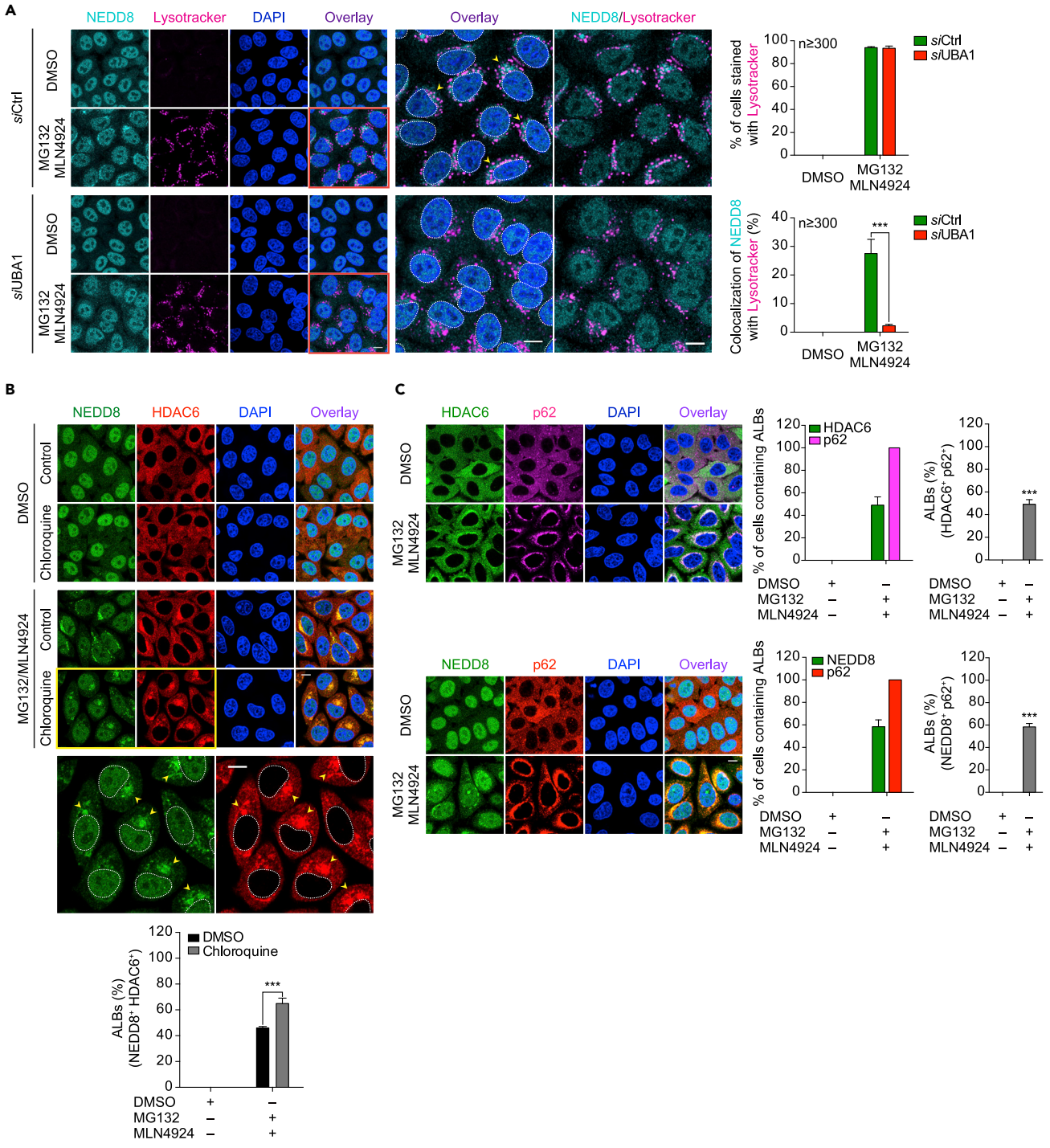

Figure 6. ALBs formation relies on autophagic pathway

(A) Similar experiment as in Figure 4A with the exception that LysoTracker was treated. Endogenous NEDD8 (cyan) and lysosome (pink) were stained with anti-NEDD8 antibody and LysoTracker (50 nM for 1 h) as indicated (left panel). Enlarge insets represent the NEDD8/lysosome colocalized-structure induced by MG132/MLN4924 in normal or knockdown of the UBA1. The colocalization of NEDD8 and lysosome was quantified as indicated (right panel). Scale bars, 10 μm.

(B) HeLa cells were treated with 50 μM Chloroquine (CQ) and followed by treatment with each reagent as indicated (upper panel). The insets show zoomed areas marked with the yellow rectangle. Arrowheads indicate ALBs condensed with NEDD8 and HDAC6. The cells containing ALBs were quantified (lower panel). Scale bars, 10 μm.

Figure 6. *Continued*

(C) HeLa cells were treated with indicated inhibitors and then followed by immunostaining with anti-p62 antibody and anti-HDAC6 (upper panel) or anti-NEDD8 (lower panel) antibodies as indicated. Cells containing ALBs were counted and quantified for analysis of colocalization between HDAC6 and p62 (lower panel). Scale bars, 10 μm.

Nuclei were counterstained with DAPI. "+" denotes positive cells showing ALBs formation with indicated markers. Data represent mean ± SEM of three independent experiments. ***$p \leq 0.01$.

See also Figure S5.

observed (Figure 5B). As shown in Figure 4, UBA1 depletion or NEDP1 overexpression can reduce ubiquitin stress-mediated NEDDylation and ALBs formation. However, a 2-fold increase in NEDDylation was observed, although ALBs formation was significantly reduced, upon tubacin treatment (Figure 5B, lower panel). These results suggest that HDAC6 controls ALBs formation through its deacetylase activity but is not involved in stress-induced NEDDylation. To further validate this observation, we knocked down HDAC6 using siRNA and analyzed the percentage of cells generating ALBs. We observed a significant reduction in ALBs formation after HDAC6 depletion (Figures 5C and 5D). Consistently, the level of stress-induced NEDDylation was increased by HDAC6 knockdown (Figure 5E). Together, these observations suggest that HDAC6 plays a crucial role in ALBs formation via its deacetylase activity, but it is not involved in stress-induced NEDDylation.

Ubiquitin stress-induced NEDDylation is coupled to aggresome-autophagy machinery

Next, we investigated which cellular signaling pathways are connected to NEDDylation-dependent ALBs formation in physiological conditions. To identify the ALBs-coupled cellular pathway, we monitored stress-induced cellular responses linked to biomolecule condensates. First, we focused on the aggresome-autophagy pathway, because HDAC6 is a major regulator of aggresome formation and cell viability in response to misfolded protein (Kawaguchi et al., 2003). We analyzed the correlation between ALBs and lysosomes using a Lysotracker probe, which is a red fluorescent dye that labels acidic organelles in live cells. As shown in Figure 6A, we observed that lysosome staining with Lysotracker is increased after MG/MLN treatment. However, the percentage of cells showing bright lysosomal staining did not change in cells with a UBA1 knockdown (Figure 6A, upper graph in right panel). Strikingly, we observed that 30% of stained lysosomes colocalized with ALBs, and this colocalization was mostly absent when UBA1 was knocked down (Figure 6A, lower graph in right panel). These results suggest that stress-induced ALBs formation is associated with lysosomal function, which is intricately linked with the aggresome-autophagy pathway. To verify whether ALBs formation is linked to autophagic processes, we analyzed ALBs formation in the absence or presence of chloroquine (CQ), which impairs autophagosome fusion with lysosomes. In the MG/MLN-treated condition, CQ increased ALBs formation and caused a dramatic structural change in the rounded cellular shape wherein ALBs are more condensed (Figure 6B). As shown Figure 5, ALB formation is dependent upon HDAC6 activity, which is required for aggresome-autophagy flux. Thus, we hypothesized that ALBs formation may be in the same pathway as the aggresome-autophagic flux. Thus, we examined whether NEDD8- and HDAC6-induced ALBs colocalized with p62, which acts as a bridge between polyubiquitinated cargo and autophagosomes via an interplay with LC3 (Ciuffa et al., 2015; Kirkin et al., 2009; Lippai and Low, 2014; Wurzer et al., 2015). To elucidate the physiological relevance of p62 and ALBs formation, co-compartmentalization between p62 and HDAC6 or NEDD8 was analyzed during ubiquitin stress (Figure 6C). We found that p62 was concentrated near ALBs and colocalized with HDAC6 and NEDD8. Furthermore, we observed that HDAC6 and NEDD8 shows approximately 50% and 60% colocalization with p62 in ALBs, respectively (Figure 6C). Next, to analyze colocalization of these three proteins, GFP-HDAC6 was transfected into cells and then co-compartmentalization between them was analyzed as in the previous experiment. We found that GFP-HDAC6 shows approximately 30% compartmentalization with NEDD8 and p62 in ALBs during ubiquitin stress (Figure S5A). These results suggest that p62 is involved in ALBs formation, and it might be connected to the aggresome-autophagic flux.

p62 is an adaptor for NEDDylation-dependent aggresome-autophagic flux

To dissect the role of p62 in ALBs formation, we investigated whether ALBs formation is affected by depletion of endogenous p62. We observed that ALBs formation does not occur when p62 is knocked down, whereas control siRNA showed no significant effects (Figure 7A). This suggests that p62 is an important factor for stress-induced ALBs formation. To understand the mechanism underlying p62-mediated ALBs formation, we analyzed whether p62 affects UBA1-mediated NEDDylation during ubiquitin stress. Interestingly, we observed no difference in NEDDylation between the siControl- and sip62-transfected cells during

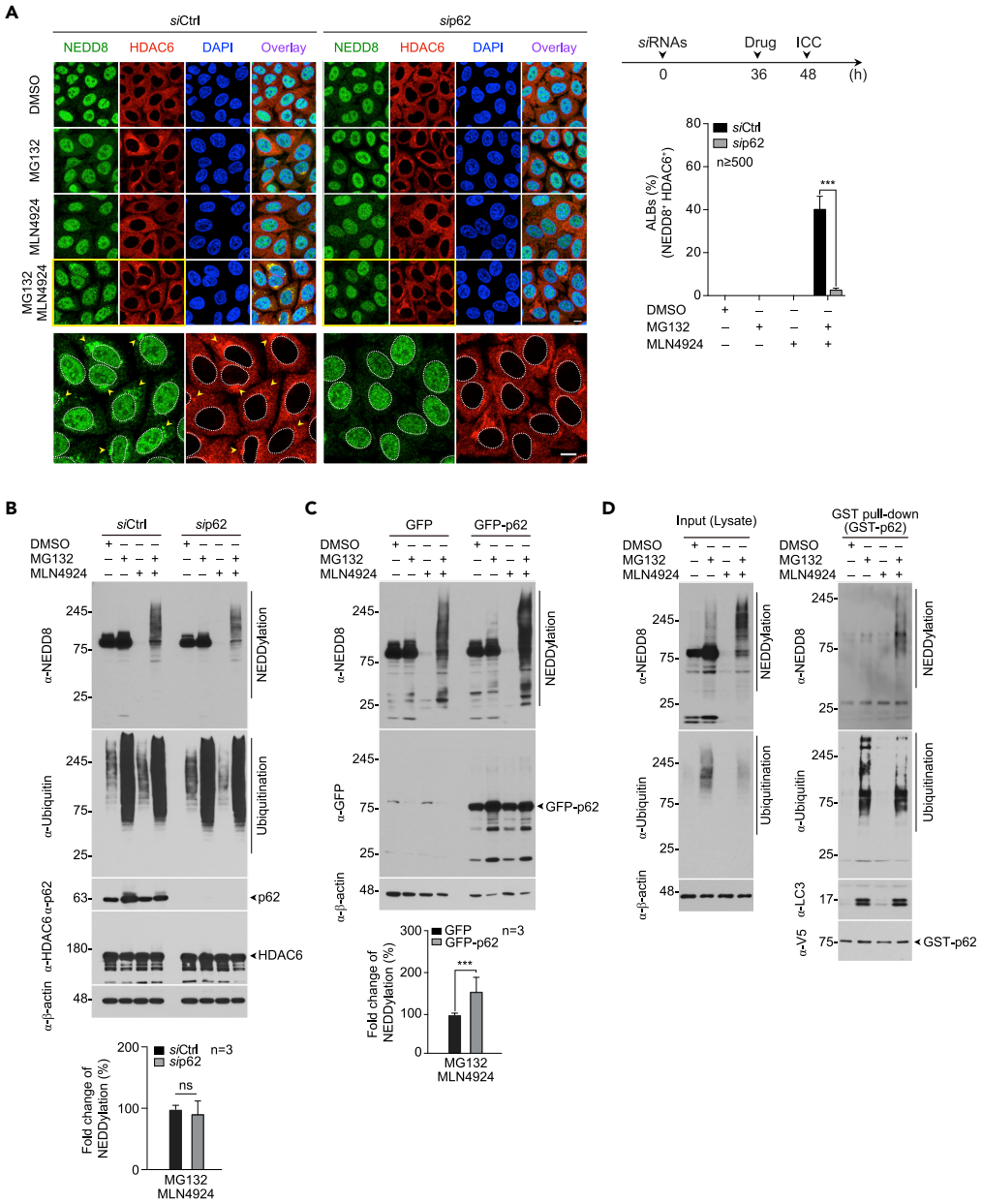

Figure 7. p62 plays as an adaptor for NEDDylated proteins under ubiquitin stress condition

(A) Cells transfected with *si*Ctrl or *si*p62 were treated with indicated inhibitors for 12 h, and then cells were fixed and stained with anti-NEDD8 and anti-HDAC6 antibodies. The insets show zoomed areas marked with the yellow rectangle. Arrowheads indicate ALBs condensed with NEDD8 and HDAC6 (left panel). The cells containing ALBs were quantified as indicated (right panel). Scale bars, 10 μm.

(B) Experiment was performed as above, and whole-cell lysates were prepared and loaded by 8%–16% SDS-PAGE. Immunoblotting analysis was performed with indicated antibodies (upper panel), and the level of NEDDylation was then quantified (lower panel).

(C) Cells were transfected with GFP or GFP-p62, and 36 h later, cells were treated with indicated inhibitors for 12 h followed by cell lysis. Cell lysates were loaded by 8%–16% SDS-PAGE and immunoblotted with indicated antibodies. NEDDylation level was then quantified as described above.

(D) HeLa cells were treated with indicated inhibitors for 12 h followed by cell lysis. Each cell extract was used for GST-p62 pull-down assay (right panel). Input (left panel) and pull-down sample with GST-p62 (right panel) were immunoblotted with indicated antibodies.

Figure 7. *Continued*
Nuclei were counterstained with DAPI. "+" denotes positive cells showing ALBs formation with indicated markers. Data represent mean ± SEM of three independent experiments. ***$p \leq 0.01$. ns, not significant.
See also Figure S5.

ubiquitin stress (Figure 7B). These data suggest that p62 may not be directly involved in UBA1-mediated NEDDylation but could be an adaptor molecule to bring NEDDylated proteins and HDAC6 together, thereby allowing ALBs formation. To further ascertain the effects of p62 on ALBs formation, GFP-p62 was transfected into HeLa cells and the effect of p62 overexpression on ALBs formation was monitored. As expected, NEDD8 colocalized with GFP-p62 and HDAC6 in ALBs (Figure S5B). In fact, p62 binds to ubiquitin and ubiquitinated proteins via its ubiquitin-associated (UBA) domain, which concentrates the ubiquitinated protein complex in the autophagosome. Consistently, we observed that GFP-p62 is colocalized with HDAC6 in cytosolic speckles, which show a similar structure to ALBs, in cells treated only with MG132 (Figure S5B). It is noteworthy that, as shown in Figure 3C, the ubiquitination of endogenous cellular proteins was increased in both MG132-treated cells and MG/MLN-treated cells, whereas NEDDylation was only detected in the latter. These results suggest that p62 and HDAC6 may have distinct roles for ubiquitin- and NEDD8-coupled cellular processes under various stress conditions. Next, we examined whether p62 overexpression affects the accumulation of NEDDylation during stress. We observed that NEDDylation was significantly increased by p62 overexpression (Figure 7C). In fact, p62 is a receptor for polyubiquitinated cargo during the autophagy process, wherein cargo is concentrated in autophagic vesicles with LC3 (Sun et al., 2018). However, it is unclear whether p62 is associated with cellular NEDDylation processes. To further demonstrate that p62 is a receptor for NEDDylated proteins, we performed GST pull-down assays using recombinant p62 and cell lysates stimulated by ubiquitin stress. NEDDylated proteins were enriched in p62 pull-down samples with LC3 proteins (Figure 7D). Further, ubiquitinated proteins generated by MG132 or MG/MLN treatment were also captured by p62 and LC3, indicating that p62 may be a NEDD8 receptor that promotes ALBs formation in the aggresome-autophagic flux linked to ubiquitin stress.

DISCUSSION

Emerging evidence indicates that the NEDD8 system is closely linked to pathological disorders of the UPS system (Kandala et al., 2014; Li et al., 2018; Soucy et al., 2010). Indeed, NEDD8 proteins are highly accumulated in ubiquitinated inclusion bodies, including neurofibrillary tangles in Alzheimer disease, Lewy bodies in Parkinson disease, and Rosenthal fibers in astrocytoma (Dil Kuazi et al., 2003; Mori et al., 2005). The presence of these inclusions normally reflects a pathological state, but the formation of the inclusion bodies likely functions as a cytoprotective mechanism rather than a pathogenic one (Bersuker et al., 2016; Moreau et al., 2010). In addition, recently, McGrail et al. reported that NEDD8 regulates the clearance of misfolded proteins in several cancers linked to deficient DNA mismatch repair (dMMR) such as microsatellite instability (MSI). In this study, they reported that dMMR/MSI tumors exhibit total proteomic instability, and NEDDylation is crucial for the removal of accumulated misfolded proteins (McGrail et al., 2020). However, the identity of signaling pathways that are involved in the formation of NEDD8-associated inclusions remains unknown. Thus, it is important to define the molecular mechanisms underlying NEDD8-mediated protein aggregation in order to understand the link between the NEDD8 system and various diseases (Enchev et al., 2015; Maghames et al., 2018).

Here, we identified HDAC6 and p62 as regulators of NEDDylation-dependent ALB formation during ubiquitin stress (Figures 5 and 7). Our data suggest that ubiquitin stress-induced NEDDylation transiently promotes the generation of cytosolic protein aggregates, thereby inducing ALB formation, which is closely linked to the aggresome-autophagy flux.

Recently, elegant proteomic and biological approaches have demonstrated that heat shock-induced NEDDylation promotes protein aggregation in the nucleus, thereby protecting the nuclear UPS from proteotoxic stress (Maghames et al., 2018). It is noteworthy that in addition to ubiquitin, the NEDD8 system is also involved in certain stress conditions to generate protein aggregates. Similarly, we show that ubiquitin depletion strongly promotes NEDD8-associated nuclear aggregation in the presence of MLN4924 (Figure 3F). In addition, we found that the simultaneous perturbation of cellular ubiquitin levels and proteasomal activity leads to nuclear protein aggregation. We also observed that MG132 treatment seems to slightly induce nuclear accumulation of NEDD8 at the nucleolus (Figures 3A, 3B, 6A, and 7A). However, our data show that MG/MLN-induced NEDDylation mainly occurs in the cytoplasm rather than in the

nucleus, suggesting that NEDDylation may respond differently depending on the type of stress. Thus, it is necessary to determine the physiological relevance of NEDDylation-dependent cytoplasmic protein aggregation. As mentioned above, previous studies have reported intense NEDD8 staining of inclusion bodies that are associated with many age-related neurodegenerative diseases (Dil Kuazi et al., 2003; Mori et al., 2005). Intriguingly, inclusion bodies containing large amounts of NEDD8 were detected in the cytoplasm but not in the nucleus. This raises the interesting possibility that pathophysiological conditions are possibly mirrored by our results. It could be argued that UBA1-mediated NEDDylation was not mimicked under physiological conditions, because we used MG132 and MLN4924 to induce ubiquitin stress in cells. However, we show that the overexpression of NEDD8 drastically induces cytosolic protein aggregation in the presence of MG132 alone (Figure 1B), suggesting that altering cellular NEDD8 homeostasis may trigger stress-induced NEDDylation similar to that triggered by NAE1 inhibitors. Consistently, Hjerpe et al. reported that NEDD8 overexpression causes UBA1-mediated NEDDylation in cells without any proteasome or NAE1 inhibition (Hjerpe et al., 2012b). In addition, proteasome activity declines during aging, and proteasomal dysfunction is associated with late-onset disorders (Saez and Vilchez, 2014). The exact mechanism underlying this dysfunction remains unclear, but the likelihood that these two phenomena occur simultaneously under certain stresses has become more apparent.

Recently, the canonical NEDD8 E2 enzymes, Ube2M and Ube2F, were shown to not be involved in UBA1-mediated NEDDylation (Hjerpe et al., 2012a). Similarly, we also demonstrate that Ube2M and Ube2F are not essential for MG/MLN-induced NEDDylation (Figure S2B), suggesting that other E2 enzymes may be involved in this pathway, as observed in another study (Hjerpe et al., 2012a). In fact, several ubiquitin E2 enzymes showed an ability to accept NEDD8 from UBA1 *in vitro*, but *in vivo* evidence remains scarce. With respect to NEDD8 conjugation to substrates, NEDD8 E3 ligases is critical to understanding the global picture of NEDD8-derived protein aggregation. In last decade, several NEDD8 E3 ligases were identified and characterized for their functional role (Embade et al., 2012; Enchev et al., 2015; Zhou et al., 2019), but so far HUWE1 is the only identified E3 ligase corresponding to NEDD8-mediated nuclear protein aggregation (Maghames et al., 2018). Although not investigated in this study, HUWE1 may not be involved in cytosolic protein aggregation under ubiquitin stress conditions. In contrast, other NEDD8 E3 ligases may be required for cytosolic protein aggregation, or NEDD8 E2 may itself be sufficient to conjugate NEDD8 to substrates without additional E3 ligases.

It has been well documented that proteotoxic stress increases UBA1-dependent NEDDylation and causes the accumulation of NEDD8/ubiquitin hybrid conjugates in the nuclear aggregates. It is to note that UBA1 utilizes both NEDD8 and ubiquitin for the initiation or extension of NEDDylation, simultaneously. Consistent with this line, we also detected ubiquitin signal from isolated NEDD8 conjugates, which are generated by MG/MLN treatment (Figure S4D). This suggests the possibility that two types of NEDD8/ubiquitin hybrid chains, mainly composed of either NEDD8 or ubiquitin, can be produced by MG/MLN treatment. As shown Figure S4D, we observed that NEDD8 from isolated NEDD8 conjugates was dramatically deconjugated by NEDP1 treatment, but ubiquitin is still conjugated without any change (Figure S4D). These data suggest that NEDD8/ubiquitin hybrid chains, which are mainly achieved by ubiquitin, still exist in the isolated NEDD8 conjugates despite the treatment of NEDP1.

Another important aspect is the nature of the observed cytoplasmic aggregates. Misfolded or aggregated proteins induced by various stresses may be targeted to different intracellular compartments, including juxtanuclear quality control compartment (JUNQ), insoluble protein deposit (IPOD), aggresome-like induced structures (ALIS), and aggresomes (Kaganovich et al., 2008; Kawaguchi et al., 2003; Kopito, 2000; Szeto et al., 2006; Takalo et al., 2013). Although aggresomes and JUNQ machinery are located close to the nucleus and contain ubiquitinated misfolded proteins, the shape and size of protein aggregates within these compartments are clearly distinct from the ALBs structure we observed. In addition, none of the cytosolic compartments has been reported to be associated with NEDD8-mediated protein aggregation. Although more studies are required to determine the nature of ALBs, our findings provide new insight into the function of NEDD8-mediated protein aggregation in various stress conditions that may be part of a pathophysiological environment.

Limitations of this study

The present study suggested that NEDD8, HDAC6, and p62 are involved in the management of proteotoxic ubiquitin stress by forming cytosolic ALBs coupled to aggresome-autophagy flux. However, precise

mechanism of ALB formation under ubiquitin stress remains to be elucidated. In addition, further studies are needed to determine the pathophysiological relevance of NEDDylation-dependent cytoplasmic protein aggregation in various diseases.

Resource availability

Lead contact

Further information and request of resources should be directed to Ho Chul Kang (hckang@ajou.ac.kr).

Material availability

All unique/stable reagents in this study are available without any restriction. Request for these reagents can be submitted to Soyeon Kim (soooooykim90@gmail.com) with a completed Materials Transfer Agreement.

Data and code availability

Octet analysis data are available at Mendeley.com (https://doi.org/10.17632/5cj2jvp9dv.1).

METHODS

All methods can be found in the accompanying Transparent methods supplemental file.

SUPPLEMENTAL INFORMATION

Supplemental information can be found online at https://doi.org/10.1016/j.isci.2021.102146.

ACKNOWLEDGMENTS

This work was supported by the National Research Foundation of Korea grant funded by the Korean government (MSIP) (No. 2020R1A2C2004988). This research was also supported by a grant for the Korea Health Technology R&D Project of the Korea Health Industry Development Institute (KHIDI) funded by the Ministry of Health & Welfare, Republic of Korea (grant number: HI16C0992).

AUTHOR CONTRIBUTIONS

The experiments were conceived and designed by S.K. and H.C.K. and mainly carried out by S.K., M.K., and Y.H.; J.Y. and S.P analyzed octet data; H.C.K. and S.K. wrote the paper.

DECLARATION OF INTERESTS

The authors declare no competing interests.

Received: September 16, 2020
Revised: January 7, 2021
Accepted: February 1, 2021
Published: March 19, 2021

REFERENCES

Amm, I., Sommer, T., and Wolf, D.H. (2014). Protein quality control and elimination of protein waste: the role of the ubiquitin-proteasome system. Biochim. Biophys. Acta *1843*, 182–196.

Bence, N.F., Sampat, R.M., and Kopito, R.R. (2001). Impairment of the ubiquitin-proteasome system by protein aggregation. Science *292*, 1552–1555.

Bennett, E.J., Bence, N.F., Jayakumar, R., and Kopito, R.R. (2005). Global impairment of the ubiquitin-proteasome system by nuclear or cytoplasmic protein aggregates precedes inclusion body formation. Mol. Cell *17*, 351–365.

Bersuker, K., Brandeis, M., and Kopito, R.R. (2016). Protein misfolding specifies recruitment to cytoplasmic inclusion bodies. J. Cell Biol. *213*, 229–241.

Chen, B., Retzlaff, M., Roos, T., and Frydman, J. (2011). Cellular strategies of protein quality control. Cold Spring Harb. Perspect. Biol. *3*, a004374.

Chhangani, D., Jana, N.R., and Mishra, A. (2013). Misfolded proteins recognition strategies of E3 ubiquitin ligases and neurodegenerative diseases. Mol. Neurobiol. *47*, 302–312.

Ciechanover, A., and Kwon, Y.T. (2015). Degradation of misfolded proteins in neurodegenerative diseases: therapeutic targets and strategies. Exp. Mol. Med. *47*, e147.

Ciechanover, A., Orian, A., and Schwartz, A.L. (2000). Ubiquitin-mediated proteolysis: biological regulation via destruction. Bioessays *22*, 442–451.

Ciuffa, R., Lamark, T., Tarafder, A.K., Guesdon, A., Rybina, S., Hagen, W.J., Johansen, T., and Sachse, C. (2015). The selective autophagy receptor p62 forms a flexible filamentous helical scaffold. Cell Rep. *11*, 748–758.

Dantuma, N.P., and Lindsten, K. (2010). Stressing the ubiquitin-proteasome system. Cardiovasc. Res. *85*, 263–271.

Deriziotis, P., Andre, R., Smith, D.M., Goold, R., Kinghorn, K.J., Kristiansen, M., Nathan, J.A., Rosenzweig, R., Krutauz, D., Glickman, M.H., et al. (2011). Misfolded PrP impairs the UPS by

interaction with the 20S proteasome and inhibition of substrate entry. EMBO J. *30*, 3065–3077.

Dikic, I. (2017). Proteasomal and autophagic degradation systems. Annu. Rev. Biochem. *86*, 193–224.

Dil Kuazi, A., Kito, K., Abe, Y., Shin, R.W., Kamitani, T., and Ueda, N. (2003). NEDD8 protein is involved in ubiquitinated inclusion bodies. J. Pathol. *199*, 259–266.

Dong, Z., and Cui, H. (2018). The autophagy-lysosomal pathways and their emerging roles in modulating proteostasis in tumors. Cells *8*, 4.

Embade, N., Fernandez-Ramos, D., Varela-Rey, M., Beraza, N., Sini, M., Gutierrez de Juan, V., Woodhoo, A., Martinez-Lopez, N., Rodriguez-Iruretagoyena, B., Bustamante, F.J., et al. (2012). Murine double minute 2 regulates Hu antigen R stability in human liver and colon cancer through NEDDylation. Hepatology *55*, 1237–1248.

Enchev, R.I., Schulman, B.A., and Peter, M. (2015). Protein neddylation: beyond cullin-RING ligases. Nat. Rev. Mol. Cell Biol. *16*, 30–44.

Gong, L., and Yeh, E.T. (1999). Identification of the activating and conjugating enzymes of the NEDD8 conjugation pathway. J. Biol. Chem. *274*, 12036–12042.

Grabbe, C., Husnjak, K., and Dikic, I. (2011). The spatial and temporal organization of ubiquitin networks. Nat. Rev. Mol. Cell Biol. *12*, 295–307.

Hanna, J., Meides, A., Zhang, D.P., and Finley, D. (2007). A ubiquitin stress response induces altered proteasome composition. Cell *129*, 747–759.

Hao, R., Nanduri, P., Rao, Y., Panichelli, R.S., Ito, A., Yoshida, M., and Yao, T.P. (2013). Proteasomes activate aggresome disassembly and clearance by producing unanchored ubiquitin chains. Mol. Cell *51*, 819–828.

Hershko, A., and Ciechanover, A. (1998). The ubiquitin system. Annu. Rev. Biochem. *67*, 425–479.

Hipp, M.S., Kasturi, P., and Hartl, F.U. (2019). The proteostasis network and its decline in ageing. Nat. Rev. Mol. Cell Biol. *20*, 421–435.

Hjerpe, R., Thomas, Y., Chen, J., Zemla, A., Curran, S., Shpiro, N., Dick, L.R., and Kurz, T. (2012a). Changes in the ratio of free NEDD8 to ubiquitin triggers NEDDylation by ubiquitin enzymes. Biochem. J. *441*, 927–936.

Hjerpe, R., Thomas, Y., and Kurz, T. (2012b). NEDD8 overexpression results in neddylation of ubiquitin substrates by the ubiquitin pathway. J. Mol. Biol. *421*, 27–29.

Kaganovich, D., Kopito, R., and Frydman, J. (2008). Misfolded proteins partition between two distinct quality control compartments. Nature *454*, 1088–1095.

Kamitani, T., Kito, K., Nguyen, H.P., and Yeh, E.T. (1997). Characterization of NEDD8, a developmentally down-regulated ubiquitin-like protein. J. Biol. Chem. *272*, 28557–28562.

Kandala, S., Kim, I.M., and Su, H. (2014). Neddylation and deneddylation in cardiac biology. Am. J. Cardiovasc. Dis. *4*, 140–158.

Kawaguchi, Y., Kovacs, J.J., McLaurin, A., Vance, J.M., Ito, A., and Yao, T.P. (2003). The deacetylase HDAC6 regulates aggresome formation and cell viability in response to misfolded protein stress. Cell *115*, 727–738.

Kim, Y.E., Hosp, F., Frottin, F., Ge, H., Mann, M., Hayer-Hartl, M., and Hartl, F.U. (2016). Soluble oligomers of PolyQ-expanded Huntingtin target a multiplicity of key cellular factors. Mol. Cell *63*, 951–964.

Kimura, Y., and Tanaka, K. (2010). Regulatory mechanisms involved in the control of ubiquitin homeostasis. J. Biochem. *147*, 793–798.

Kirkin, V., McEwan, D.G., Novak, I., and Dikic, I. (2009). A role for ubiquitin in selective autophagy. Mol. Cell *34*, 259–269.

Kocaturk, N.M., and Gozuacik, D. (2018). Crosstalk between mammalian autophagy and the ubiquitin-proteasome system. Front. Cell Dev. Biol. *6*, 128.

Komander, D., and Rape, M. (2012). The ubiquitin code. Annu. Rev. Biochem. *81*, 203–229.

Kopito, R.R. (2000). Aggresomes, inclusion bodies and protein aggregation. Trends Cell Biol. *10*, 524–530.

Lee, B.H., Lu, Y., Prado, M.A., Shi, Y., Tian, G., Sun, S., Elsasser, S., Gygi, S.P., King, R.W., and Finley, D. (2016). USP14 deubiquitinates proteasome-bound substrates that are ubiquitinated at multiple sites. Nature *532*, 398–401.

Lee, J.Y., Koga, H., Kawaguchi, Y., Tang, W., Wong, E., Gao, Y.S., Pandey, U.B., Kaushik, S., Tresse, E., Lu, J., et al. (2010). HDAC6 controls autophagosome maturation essential for ubiquitin-selective quality-control autophagy. EMBO J. *29*, 969–980.

Leidecker, O., Matic, I., Mahata, B., Pion, E., and Xirodimas, D. (2012). The ubiquitin E1 enzyme Ube1 mediates NEDD8 activation under diverse stress conditions. Cell Cycle *11*, 1142–1150.

Li, J., Johnson, J.A., and Su, H. (2018). Ubiquitin and Ubiquitin-like proteins in cardiac disease and protection. Curr. Drug Targets *19*, 989–1002.

Li, J., Ma, W., Li, H., Hou, N., Wang, X., Kim, I.M., Li, F., and Su, H. (2015). NEDD8 ultimate buster 1 long (NUB1L) protein suppresses atypical neddylation and promotes the proteasomal degradation of misfolded proteins. J. Biol. Chem. *290*, 23850–23862.

Lilienbaum, A. (2013). Relationship between the proteasomal system and autophagy. Int. J. Biochem. Mol. Biol. *4*, 1–26.

Limanaqi, F., Biagioni, F., Gambardella, S., Familiari, P., Frati, A., and Fornai, F. (2020). Promiscuous roles of autophagy and proteasome in neurodegenerative proteinopathies. Int. J. Mol. Sci. *21*, 3028.

Lindersson, E., Beedholm, R., Hojrup, P., Moos, T., Gai, W., Hendil, K.B., and Jensen, P.H. (2004). Proteasomal inhibition by alpha-synuclein filaments and oligomers. J. Biol. Chem. *279*, 12924–12934.

Lippai, M., and Low, P. (2014). The role of the selective adaptor p62 and ubiquitin-like proteins in autophagy. Biomed. Res. Int. *2014*, 832704.

Lorenzo, A., and Yankner, B.A. (1996). Amyloid fibril toxicity in Alzheimer's disease and diabetes. Ann. N. Y. Acad. Sci. *777*, 89–95.

Maghames, C.M., Lobato-Gil, S., Perrin, A., Trauchessec, H., Rodriguez, M.S., Urbach, S., Marin, P., and Xirodimas, D.P. (2018). NEDDylation promotes nuclear protein aggregation and protects the Ubiquitin Proteasome System upon proteotoxic stress. Nat. Commun. *9*, 4376.

McGrail, D.J., Garnett, J., Yin, J., Dai, H., Shih, D.J.H., Lam, T.N.A., Li, Y., Sun, C., Li, Y., Schmandt, R., et al. (2020). Proteome instability is a therapeutic vulnerability in mismatch repair-deficient cancer. Cancer Cell *37*, 371–386.e12.

Moreau, K., Luo, S., and Rubinsztein, D.C. (2010). Cytoprotective roles for autophagy. Curr. Opin. Cell Biol. *22*, 206–211.

Mori, F., Nishie, M., Piao, Y.S., Kito, K., Kamitani, T., Takahashi, H., and Wakabayashi, K. (2005). Accumulation of NEDD8 in neuronal and glial inclusions of neurodegenerative disorders. Neuropathol. Appl. Neurobiol. *31*, 53–61.

Ouyang, H., Ali, Y.O., Ravichandran, M., Dong, A., Qiu, W., MacKenzie, F., Dhe-Paganon, S., Arrowsmith, C.H., and Zhai, R.G. (2012). Protein aggregates are recruited to aggresome by histone deacetylase 6 via unanchored ubiquitin C termini. J. Biol. Chem. *287*, 2317–2327.

Park, C.W., and Ryu, K.Y. (2014). Cellular ubiquitin pool dynamics and homeostasis. BMB Rep. *47*, 475–482.

Peng, H., Yang, J., Li, G., You, Q., Han, W., Li, T., Gao, D., Xie, X., Lee, B.H., Du, J., et al. (2017). Ubiquitylation of p62/sequestosome1 activates its autophagy receptor function and controls selective autophagy upon ubiquitin stress. Cell Res. *27*, 657–674.

Petroski, M.D., and Deshaies, R.J. (2005). Function and regulation of cullin-RING ubiquitin ligases. Nat. Rev. Mol. Cell Biol. *6*, 9–20.

Ross, C.A., and Poirier, M.A. (2004). Protein aggregation and neurodegenerative disease. Nat. Med. *10 Suppl*, S10–S17.

Saez, I., and Vilchez, D. (2014). The mechanistic links between proteasome activity, aging and age-related diseases. Curr. Genomics *15*, 38–51.

Schipper-Krom, S., Juenemann, K., and Reits, E.A. (2012). The ubiquitin-proteasome system in Huntington's disease: are proteasomes impaired, initiators of disease, or coming to the rescue? Biochem. Res. Int. *2012*, 837015.

Schubert, U., Anton, L.C., Gibbs, J., Norbury, C.C., Yewdell, J.W., and Bennink, J.R. (2000). Rapid degradation of a large fraction of newly synthesized proteins by proteasomes. Nature *404*, 770–774.

Soucy, T.A., Dick, L.R., Smith, P.G., Milhollen, M.A., and Brownell, J.E. (2010). The NEDD8

conjugation pathway and its relevance in cancer biology and therapy. Genes Cancer *1*, 708–716.

Sun, D., Wu, R., Zheng, J., Li, P., and Yu, L. (2018). Polyubiquitin chain-induced p62 phase separation drives autophagic cargo segregation. Cell Res. *28*, 405–415.

Szeto, J., Kaniuk, N.A., Canadien, V., Nisman, R., Mizushima, N., Yoshimori, T., Bazett-Jones, D.P., and Brumell, J.H. (2006). ALIS are stress-induced protein storage compartments for substrates of the proteasome and autophagy. Autophagy *2*, 189–199.

Takahashi, M., Kitaura, H., Kakita, A., Kakihana, T., Katsuragi, Y., Nameta, M., Zhang, L., Iwakura, Y., Nawa, H., Higuchi, M., et al. (2018). USP10 is a driver of ubiquitinated protein aggregation and aggresome formation to inhibit apoptosis. iScience *9*, 433–450.

Takalo, M., Salminen, A., Soininen, H., Hiltunen, M., and Haapasalo, A. (2013). Protein aggregation and degradation mechanisms in neurodegenerative diseases. Am. J. Neurodegener. Dis. *2*, 1–14.

Taylor, J.P., Hardy, J., and Fischbeck, K.H. (2002). Toxic proteins in neurodegenerative disease. Science *296*, 1991–1995.

Treusch, S., Cyr, D.M., and Lindquist, S. (2009). Amyloid deposits: protection against toxic protein species? Cell Cycle *8*, 1668–1674.

Vilchez, D., Saez, I., and Dillin, A. (2014). The role of protein clearance mechanisms in organismal ageing and age-related diseases. Nat. Commun. *5*, 5659.

Wada, H., Kito, K., Caskey, L.S., Yeh, E.T., and Kamitani, T. (1998). Cleavage of the C-terminus of NEDD8 by UCH-L3. Biochem. Biophys. Res. Commun. *251*, 688–692.

Wang, C., and Wang, X. (2015). The interplay between autophagy and the ubiquitin-proteasome system in cardiac proteotoxicity. Biochim. Biophys. Acta *1852*, 188–194.

Whitby, F.G., Xia, G., Pickart, C.M., and Hill, C.P. (1998). Crystal structure of the human ubiquitin-like protein NEDD8 and interactions with ubiquitin pathway enzymes. J. Biol. Chem. *273*, 34983–34991.

Wickstrom, S.A., Masoumi, K.C., Khochbin, S., Fassler, R., and Massoumi, R. (2010). CYLD negatively regulates cell-cycle progression by inactivating HDAC6 and increasing the levels of acetylated tubulin. EMBO J. *29*, 131–144.

Wu, K., Yamoah, K., Dolios, G., Gan-Erdene, T., Tan, P., Chen, A., Lee, C.G., Wei, N., Wilkinson, K.D., Wang, R., et al. (2003). DEN1 is a dual function protease capable of processing the C terminus of Nedd8 and deconjugating hyper-neddylated CUL1. J. Biol. Chem. *278*, 28882–28891.

Wurzer, B., Zaffagnini, G., Fracchiolla, D., Turco, E., Abert, C., Romanov, J., and Martens, S. (2015). Oligomerization of p62 allows for selection of ubiquitinated cargo and isolation membrane during selective autophagy. Elife *4*, e08941.

Zhou, L., Jiang, Y., Luo, Q., Li, L., and Jia, L. (2019). Neddylation: a novel modulator of the tumor microenvironment. Mol. Cancer *18*, 77.

iScience, Volume *24*

Supplemental Information

Stress-induced NEDDylation promotes cytosolic protein aggregation through HDAC6 in a p62-dependent manner

Soyeon Kim, Mira Kwon, Yiseul Hwang, Junghyun Yoon, Sangwook Park, and Ho Chul Kang

Figure S1

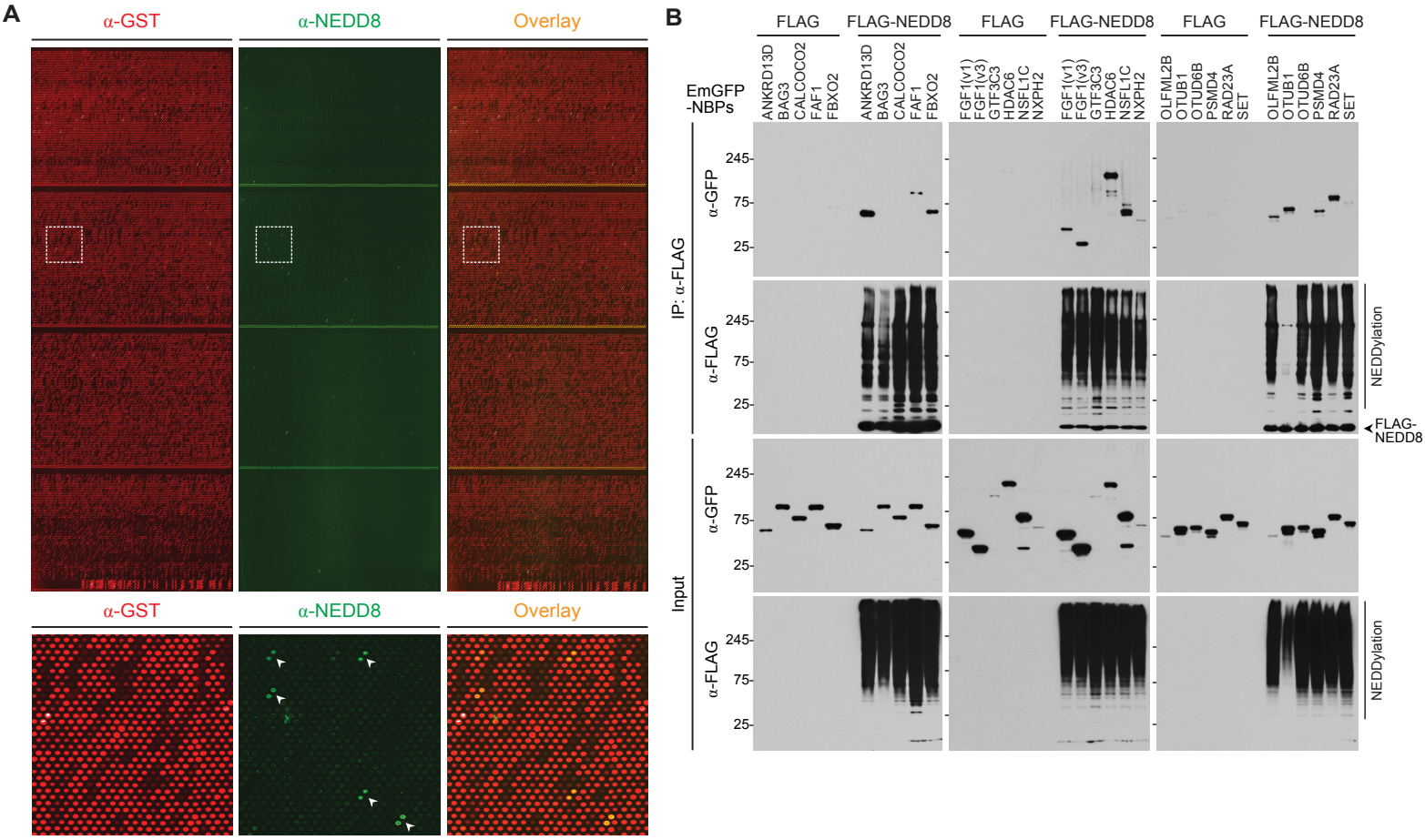
A
α-GST
α-NEDD8
Overlay
α-GST
α-NEDD8
Overlay
B
FLAG
FLAG-NEDD8
FLAG
FLAG-NEDD8
FLAG
FLAG-NEDD8
EmGFP
-NBPs
ANKRD13D
BAG3
CALCOCO2
FAF1
FBXO2
ANKRD13D
BAG3
CALCOCO2
FAF1
FBXO2
FGF1(v1)
FGF1(v3)
GTF3C3
HDAC6
NSFL1C
NXPH2
FGF1(v1)
FGF1(v3)
GTF3C3
HDAC6
NSFL1C
NXPH2
OLFML2B
OTUB1
OTUD6B
PSMD4
RAD23A
SET
OLFML2B
OTUB1
OTUD6B
PSMD4
RAD23A
SET
IP: α-FLAG
α-GFP
245
75
25
α-FLAG
245
75
25
NEDDylation
FLAG-
NEDD8
Input
α-GFP
245
75
25
α-FLAG
245
75
25
NEDDylation

Figure S2

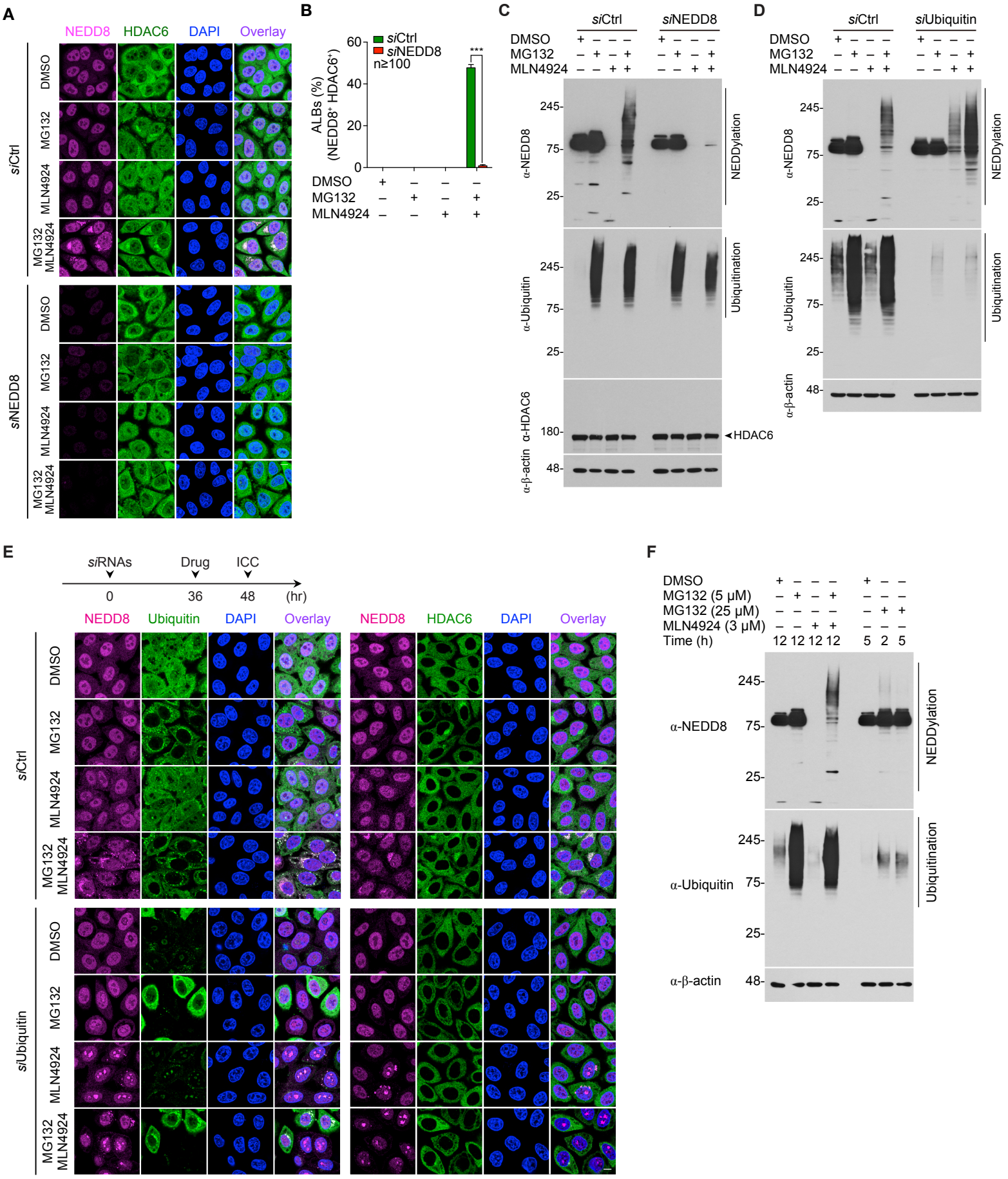
A
NEDD8
HDAC6
DAPI
Overlay
siCtrl
siNEDD8
DMSO
MG132
MLN4924
MG132 MLN4924
B
siCtrl
siNEDD8
n≥100
***
ALBs (%) (NEDD8+ HDAC6+)
60
40
20
0
DMSO
MG132
MLN4924
C
siCtrl
siNEDD8
DMSO
MG132
MLN4924
α-NEDD8
α-Ubiquitin
α-HDAC6
α-β-actin
245
75
25
180
48
NEDDylation
Ubiquitination
HDAC6
D
siCtrl
siUbiquitin
α-NEDD8
α-Ubiquitin
α-β-actin
NEDDylation
Ubiquitination
E
siRNAs
Drug
ICC
0
36
48
(hr)
NEDD8
Ubiquitin
DAPI
Overlay
HDAC6
siCtrl
siUbiquitin
F
DMSO
MG132 (5 μM)
MG132 (25 μM)
MLN4924 (3 μM)
Time (h)
12 12 12 12 5 2 5
α-NEDD8
α-Ubiquitin
α-β-actin
NEDDylation
Ubiquitination

Figure S3

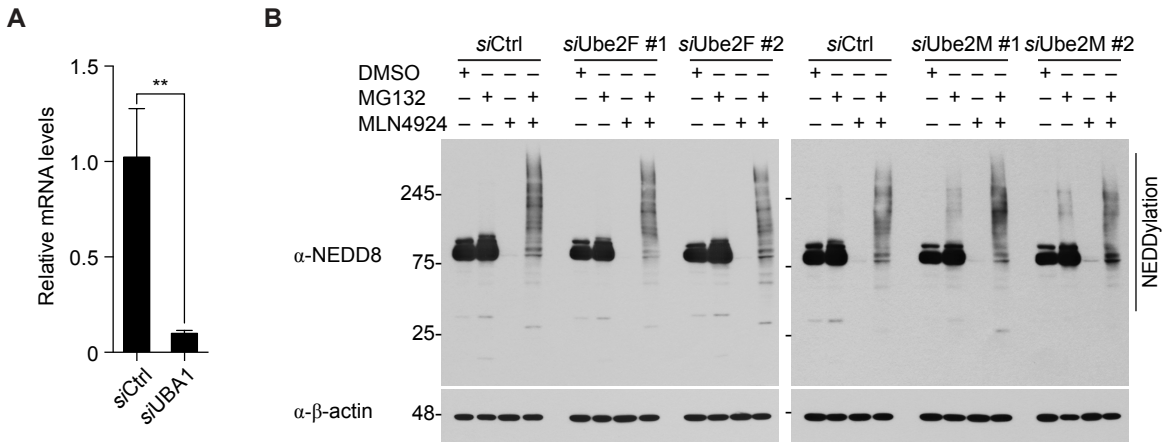
A
Relative mRNA levels
1.5
1.0
0.5
0
**
siCtrl
siUBA1
B
siCtrl
siUbe2F #1
siUbe2F #2
siCtrl
siUbe2M #1
siUbe2M #2
DMSO
MG132
MLN4924
α-NEDD8
245-
75-
25-
α-β-actin
48-
NEDDylation

Figure S4

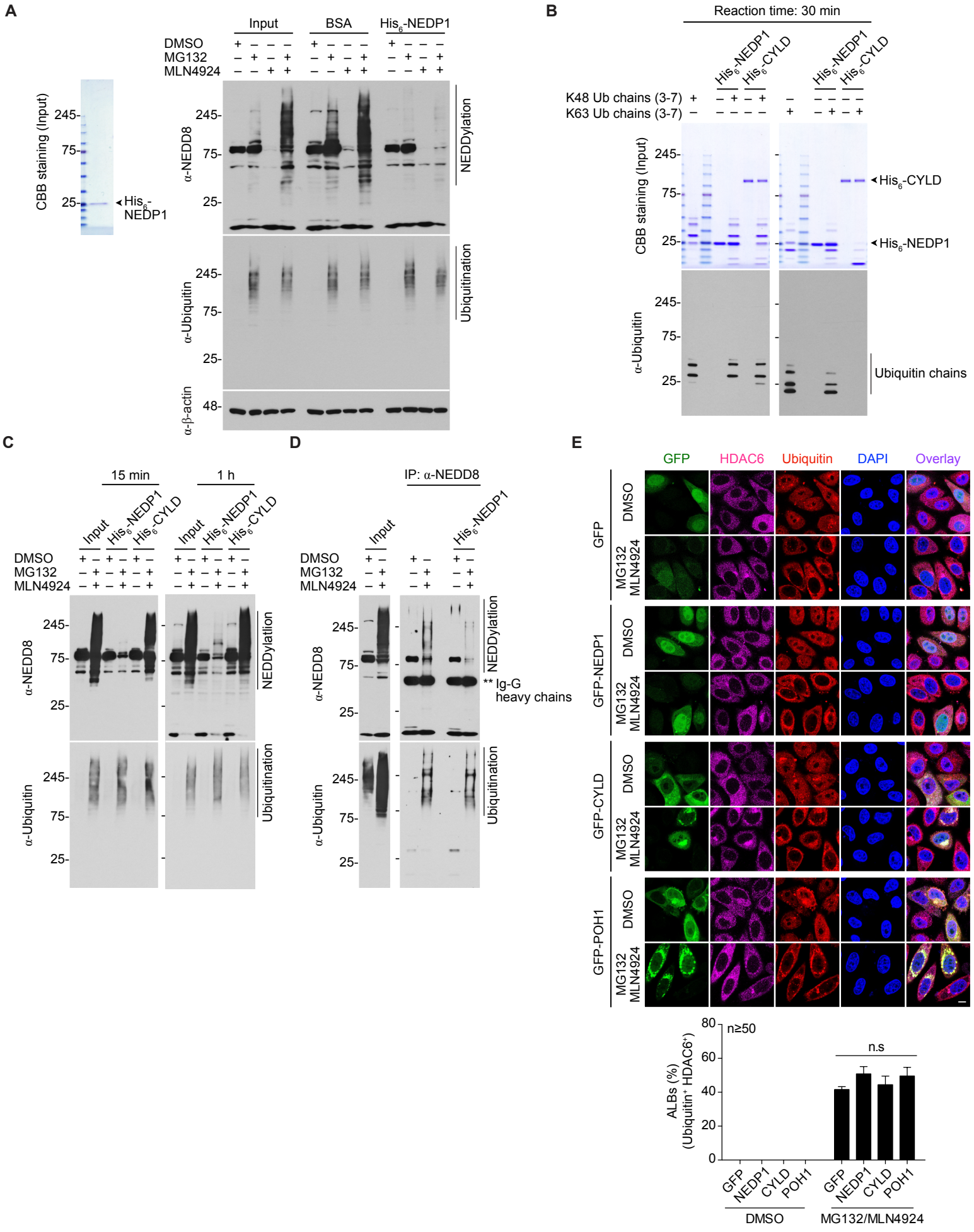
A
Input
BSA
His6-NEDP1
DMSO
MG132
MLN4924
CBB staining (Input)
245
75
25
His6-NEDP1
α-NEDD8
NEDDylation
α-Ubiquitin
Ubiquitination
α-β-actin
48
B
Reaction time: 30 min
His6-NEDP1
His6-CYLD
K48 Ub chains (3-7)
K63 Ub chains (3-7)
CBB staining (Input)
α-Ubiquitin
Ubiquitin chains
C
15 min
1 h
Input
D
IP: α-NEDD8
** Ig-G heavy chains
E
GFP
HDAC6
Ubiquitin
DAPI
Overlay
GFP
GFP-NEDP1
GFP-CYLD
GFP-POH1
DMSO
MG132 MLN4924
ALBs (%) (Ubiquitin+ HDAC6+)
n≥50
n.s
NEDP1
CYLD
POH1
MG132/MLN4924

Figure S5

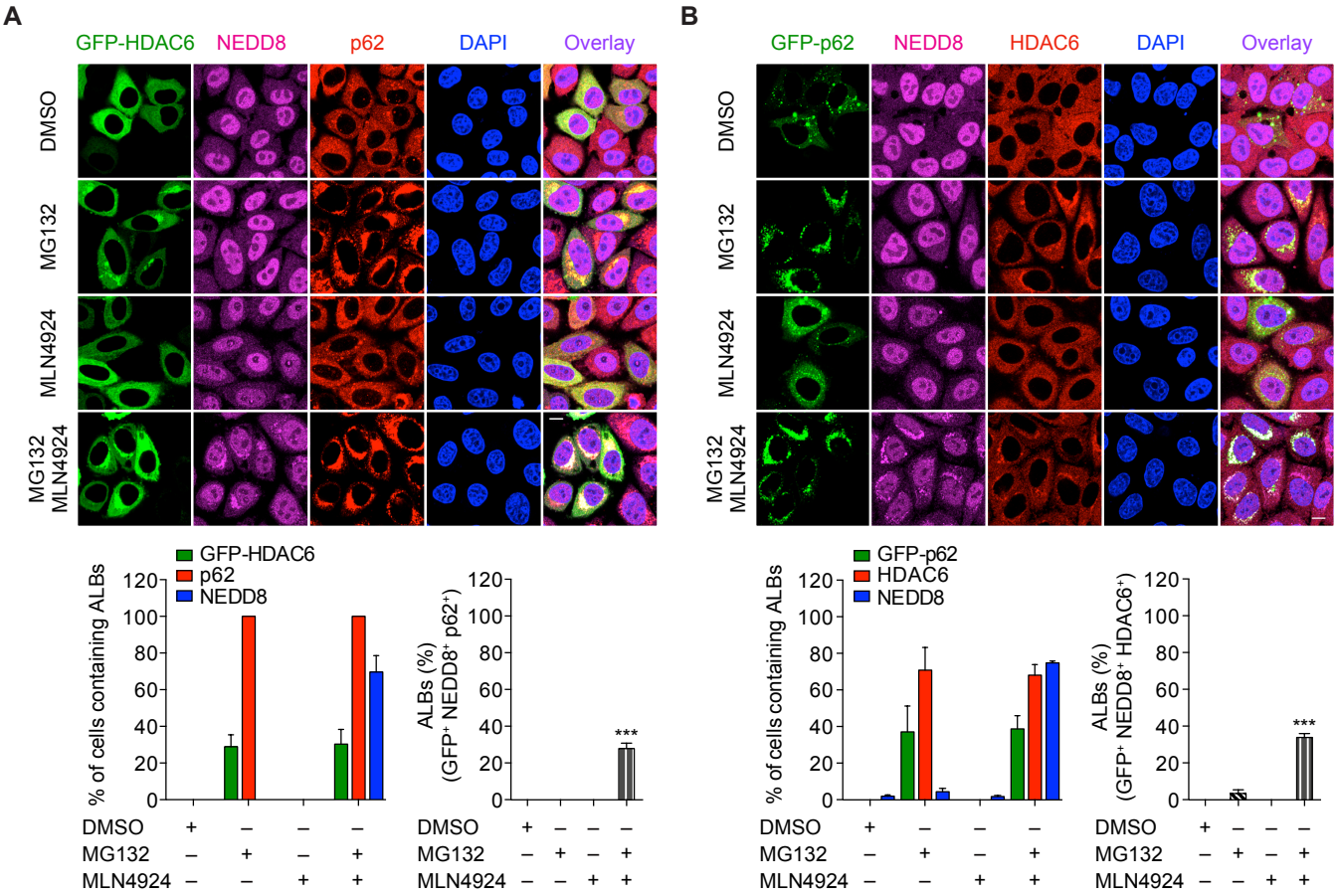
A
GFP-HDAC6
NEDD8
p62
DAPI
Overlay
DMSO
MG132
MLN4924
MG132 MLN4924
GFP-HDAC6
p62
NEDD8
% of cells containing ALBs
ALBs (%) (GFP+ NEDD8+ p62+)
***
DMSO
MG132
MLN4924
B
GFP-p62
NEDD8
HDAC6
DAPI
Overlay
GFP-p62
HDAC6
NEDD8
% of cells containing ALBs
ALBs (%) (GFP+ NEDD8+ HDAC6+)
***

Figure S1. Identification of NEDD8 binding proteins using a human protein microarray, related to Figure 1.

(A) Recombinant NEDD8 protein (2 μg/mL) was applied on HuProt^{TM} 3.0 protein microarray as described in Transparent Methods. NEDD8 binding proteins (green) were detected by anti-Rabbit Alexa Flour 647 and scanned by GenePix 4000B (Molecular Devices). Signal intensity for each spot was obtained as the ratio of foreground to background signals and was normalized with the GST signal intensity (red). The mean signal intensity of each protein on the protein array was calculated. The insets show zoomed areas marked with the white rectangle. Arrowheads indicate postulated NEDD8 binding proteins.

(B) The indicated plasmids were transfected into HEK293FT cells. Cell extracts were immunoprecipitated with anti-FLAG M2 antibody immobilized on agarose and then immunoblotted with the indicated antibodies.

Figure S2. NEDD8 directly controls cytosolic ALBs formation, related to Figure 3.

(A-C) HeLa cells were transfected with *si*Ctrl or *si*NEDD8 and then treated with reagents as indicated. After 48 h, cells were stained with anti-NEDD8 and anti-HDAC6 antibodies (A), and the cells containing ALBs were quantified (B). Experiment performed as above and whole cell lysates were prepared and loaded by 8-16% SDS-PAGE. Immunoblotting analysis was performed with indicated antibodies (C).

(D and E) Similar experiments as in B with the exception that *si*Ctrl or *si*Ubiquitin (combination of siRNAs for RPS27A or UBA52) were transfected. Cell lysates derived from above experiment were subjected into immunoblotting analysis with anti-NEDD8 and anti-Ubiquitin antibodies (D). Endogenous NEDD8 (pink), ubiquitin (green) or HDAC6 (green) was visualized by immunostaining as indicated (E).

(F) HeLa cells were treated with DMSO, MLN4924 (3 μM), MG132 (5 μM or 25 μM) as single or in combination during indicated time. Scale bars, 10 μm.

Nuclei were counterstained with DAPI. + sign denotes positive cells showing ALBs formation with indicated markers. Data represent mean ± SEM of three independent experiments. ***$P \leq 0.01$.

Figure S3. Classical NEDD8-E2 enzymes are not required for stress-induced NEDDylation, related to Figure 4.

(A) Cells were transfected with *si*Ctrl or *si*UBA1, and then mRNA levels of *UBA* gene was confirmed by quantitative real-time PCR.

(B) Cells transfected with *si*Ctrl or *si*NEDD8 E2s (Ube2F and Ube2M) were treated with indicated inhibitors for 12 h, followed by cell lysis. Cell lysates were loaded by 8-16% SDS-PAGE and immunoblotting analysis was performed with indicated antibodies.

Data represent mean ± SEM of three independent experiments. $^{**}P \leq 0.05$.

Figure S4. Stress-induced ALBs formation is mainly achieved by NEDDylation rather than ubiquitination, related to Figure 4.

(A) HeLa cells were treated with indicated inhibitors for 12 h, followed by cell lysis. Each cell lysate was used for deNEDDylation assay with His_6-tagged-NEDP1 (His_6-NEDP1) as described in Transparent Methods. After deNEDDylation assay, samples were immunoblotted with indicated antibodies (right panel). The purity of His_6-NEDP1 applied on deNEDDylation assay was checked by staining with Coomassie Brilliant Blue (left panel). Data are representative of three independent experiments.

(B) *In vitro* deubiquitination assay was performed with recombinant NEDP1 or CYLD in the presence of recombinant ubiquitin chains as indicated. The purity of recombinant proteins was visualized by staining with Coomassie Brilliant Blue and their enzymatic activity was accessed by immunoblotting with anti-ubiquitin antibody.

(C) Similar experiments as in B with the exception that cell lysates were used instead of ubiquitin chains for the assay during indicated time. After deNEDDylation assay, samples were immunoblotted with indicated antibodies.

(D) HeLa cells were treated with indicated inhibitors for 12 h, followed by cell lysis. Each cell lysate was used for immunoprecipitation assay to isolate NEDDylated proteins. Purified NEDDylated proteins were subjected into *in vitro* deNEDDylation assay with His_6-NEDP1 as indicated. Input (left panel) and deNEDDylation samples were immunoblotted with indicated antibodies.

(E) The indicated plasmids were transfected into HeLa cells and then treated with DMSO or MG/MLN for 12 h. After 48 h, each cell was fixed and immunostained with indicated antibodies

(Upper panel). The cells containing HDAC6/ubiquitin-colocalized structure were counted for quantification (Lower panel). Scale bars, 10 μm.

Nuclei were counterstained with DAPI. + sign denotes positive cells showing ALBs formation with indicated markers. Data represent mean ± SEM of three independent experiments. ns, not significant.

Figure S5. HDAC6 and p62 have distinct roles for NEDD8 and ubiquitin under stress conditions, related to Figure 6 and Figure 7.

(A) GFP-HDAC6 was transfected into HeLa cells and then treated with indicated reagents for 12 h. After 48 h, each cell was fixed and immunostained with indicated antibodies (Upper panel). The cells containing GFP-HDAC6/p62/ubiquitin-colocalized structure were counted for quantification (lower panel).

(B) GFP-p62 was transfected into HeLa cells and then treated with indicated reagents for 12 h. After 48 h, each cell was fixed and immunostained with indicated antibodies (Upper panel). The cells containing GFP-p62/HDAC6/NEDD8-colocalized structure were counted for quantification (lower panel).

Nuclei were counterstained with DAPI. + sign denotes positive cells showing ALBs formation with indicated markers. Data represent mean ± SEM of three independent experiments. ***$P \leq 0.01$.

Table S1. Plasmids list, Related to Methods

Plasmids	Source	Catalog No.
pcDNA6.2/N term-EmGFP-ANKRD13D	This study	N/A
pcDNA6.2/N term-EmGFP-BAG3	This study	N/A
pcDNA6.2/N term-EmGFP-CALCOCO2	This study	N/A
pcDNA6.2/N term-EmGFP-FAF1	This study	N/A
pcDNA6.2/N term-EmGFP-FBXO2	This study	N/A
pcDNA6.2/N term-EmGFP-FGF1 (v1)	This study	N/A
pcDNA6.2/N term-EmGFP-FGF1 (v3)	This study	N/A
pcDNA6.2/N term-EmGFP-GTF3C3	This study	N/A
pcDNA6.2/N term-EmGFP-HDAC6	This study	N/A
pcDNA6.2/N term-EmGFP-NSFL1C	This study	N/A
pcDNA6.2/N term-EmGFP-NXPH2	This study	N/A
pcDNA6.2/N term-EmGFP-OLFML2B	This study	N/A
pcDNA6.2/N term-EmGFP-OTUB1	This study	N/A
pcDNA6.2/N term-EmGFP-OTUD6B	This study	N/A
pcDNA6.2/N term-EmGFP-PSMD4	This study	N/A
pcDNA6.2/N term-EmGFP-RAD23A	This study	N/A
pcDNA6.2/N term-EmGFP-SET	This study	N/A
362 pCS Cherry-NEDD8	This study	N/A
FLAG-NEDD8 WT	This study	N/A
FLAG-NEDD8 $G^{75/76}A$	This study	N/A
pcDNA3.1/n-V5-NEDD8 WT	This study	N/A
pcDNA3.1/n-V5-NEDD8 $G^{75/76}A$	This study	N/A
pcDNA3.1/n-V5-NEDD8 $G^{77/78}A$	This study	N/A
pcDNA3.1/n-V5-NEDD8 $G^{75\sim78}A$	This study	N/A
pcDNA-HDAC6-FLAG	Addgene	#30482
pDEST53-NEDP1	This study	N/A
pDEST53-CYLD	This study	N/A
pDEST53-POH1	This study	N/A
pDEST53-USP10	This study	N/A
pDEST53-p62	This study	N/A
pDEST20 (GST only)	This study	N/A
pDEST20-NEDD8 WT	This study	N/A
pDEST20-3C-NEDD8 WT	This study	N/A
pDEST20-3C-NEDD8 $G^{75/76}A$	This study	N/A
pDEST20-3C-NEDD8 $G^{77/78}A$	This study	N/A
pDEST20-3C-NEDD8 $G^{75\sim78}A$	This study	N/A
pDEST20-HDAC6	This study	N/A
pDEST20-3C/V5-HDAC6	This study	N/A
pDEST20-3C/V5-p62	This study	N/A

Table S2. Primers and siRNAs list, Related to Methods

Plasmids	Forward primers	Reverse primers	Reference	Supplier (http://www.genolution1.com)
NEDD8 $G^{75/76}A$	5'-TCT GAG AGC AGC AGG TGG TCT TAG-3'	5'-CTA AGA CCA CCT GCT GCT CTC AGA-3'	In this study	Genolution
NEDD8 $G^{77/78}A$	5'-TCT GAG AGG AGG AGC GGC GCT TAG GCA GTA-3'	5'-CTA CTG CCT AAG CGC CGC TCC TCC TCT CAG A-3'	In this study	Genolution
NEDD8 $G^{75-78}A$	5'-TCT GAG AGC AGC AGC GGC GCT TAG GCA G-3'	5'-CTG CCT AAG CGC CGC TGC TGC TCT CAG A-3'	In this study	Genolution
Target Gene	**siRNA Sequences**	**Targeting region**	**Reference**	**Supplier (http://www.genolution1.com)**
Negative control	5'-CCUCGUGCCGUUCCAUCAGGUAG-3'	-	In this study	Genolution
NEDD8	5'-GCUUCCCUCUCUUAUGACU-3'	3' UTR	doi:10.4049/jimmunol.1501752	Genolution
HDAC6	5'-GAAACAACCCAGUACAUGA-3'	CDS	In this study	Genolution
p62	5'-GCAUUGAAGUUGAUAUCGAU-3'	CDS	https://doi.org/10.1016/j.molcel.2017.10.029	Genolution
UBA1	5'-GATGAGGGCTTCTACAAGA-3'	CDS	https://doi.org/10.1016/j.molcel.2011.05.034	Genolution
Ube2F #1	5'-GGAATAAAGTGGATGACTA-3'	CDS	DOI: 10.1038/ncb3260	Genolution
Ube2F #2	5'-CAACATAAATACAGCAAGA-3'	3'UTR	DOI: 10.1038/ncb3260	Genolution
Ube2M #1	5'-GATGAGGGCTTCTACAAGA-3'	CDS	DOI: 10.1038/ncb3260	Genolution
Ube2M #2	5'-AGCCAGTCCTTACGATAAA-3'	CDS	doi:10.1128/MCB.05496-11	Genolution
NEDP1	5'-CAGAGAAACUGGAGGCUUU-3'	CDS	https://doi.org/10.1038/onc.2009.314	Genolution
UBA52	5'-UUGACAUUCUCAAUGGUGU-3'	CDS	In this study	Genolution
RPS27A	5'-AGGCCAAGAUCCAGGAUAA-3'	CDS	https://doi.org/10.1016/j.cell.2013.08.029	Genolution

Table S3. Proteins list, Related to Methods

Recombinant Proteins	Source	Catalog No./Purified proteins
His6-NEDP1/SENP8	Boston Biochem	E-800
His6-CYLD, isoform 1, human recombinant	BostonBiochem	E-556
Poly-Ubiquitin/Ub3-Ub7 WT Chains (K48-linked)	BostonBiochem	UC-220
Poly-Ubiquitin/Ub3-Ub7 WT Chains (K63-linked)	BostonBiochem	UC-320
Recombinant GST	This study	purified from Sf9 cells
Recombinant GST-NEDD8 WT protein	This study	purified from Sf9 cells
Recombinant NEDD8 $G^{75/76}A$ protein	This study	purified from Sf9 cells
Recombinant NEDD8 $G^{77/78}A$ protein	This study	purified from Sf9 cells
Recombinant NEDD8 $G^{75\sim78}A$ protein	This study	purified from Sf9 cells
Recombinant GST-3C/V5-p62 protein	This study	purified from Sf9 cells
Recombinant GST-HDAC6 protein	This study	purified from Sf9 cells
Recombinant V5-HDAC6 protein	This study	purified from Sf9 cells

Table S4. Antibodies list, Related to Methods

Antibodies	Source	Catalog No.	Immunoblot/ Immunoprecipiation*	IF/Microarray**
NEDD8 antibody [Y297]	GeneTex	GTX61205	1:1,000	1:1,000**
Anti-NEDD8 antibody [Y297] (ab81264)	Abcam	ab81264	1:1,000/1 µg*	1:500
Polyclonal Rabbit anti-Ubiquitin antibody	DAKO	Z0458	1:1,000	1:500
Anti-Ubiquitinylated proteins Antibody, clone FK2	Millipore	04-263	-	1:500
mono- and polyubiquitin antibody, FK2	Bio-Rad	MCA6035	-	1:500
Monoclonal Anti-Ubiquitin antibody produced in mouse	Sigma-Aldrich	U0508	1:1,000	-
HDAC6 antibody [4C5]	GeneTex	GTX84377	1:2,000	1:500
HDAC6 (D2E5) Rabbit mAb	Cell Signaling Technology	7558S	1:2,000	1:200
LC3A/B (D3U4C) XP® Rabbit mAb #12741	Cell Signaling Technology	12741	1:1,000	-
Anti-SQSTM1 / p62 antibody (ab56416)	Abcam	ab56416	1:2,000	1:1,000
Anti-p62 (SQSTM1) (Human) pAb (Polyclonal Antibody)	MBL	PM045	-	1:1,000
acetylated α Tubulin (6-11B-1)	Santa Cruz	sc-23950	1:5,000	-
Anti-GFP antibody	Abcam	ab6556	1:5,000	-
Anti-Glutathione-S-Transferase Antibody, S. japonicum form	Millipore	AB3282	1:2,000	-
Anti-Glutathione-S-transferase (GST) antibody, Mouse monoclonal	Sigma-Aldrich	SAB4200237	-	1:5,000
ANTI-FLAG® M2 Affinity Gel*	Sigma-Aldrich	A2220	1 µg*	-
Monoclonal ANTI-FLAG® M2-Peroxidase (HRP)	Sigma-Aldrich	A8592	1:2,000	-
Monoclonal ANTI-FLAG® M2 antibody produced in mouse	Sigma-Aldrich	F1804-50UG	-	1:1,000
Monoclonal Anti-V5-Peroxidase antibody produced in mouse, clone V5-10	Sigma-Aldrich	V2260	1:4,000	-
Anti-beta Actin antibody [AC-15]	Abcam	ab6276	1:10,000	-
Anti-mouse IgG, HRP-linked Antibody	Cell Signaling Technology	7076	1:5,000	-
Peroxidase AffiniPure Goat Anti-Rabbit IgG (H+L)	Jackson ImmunoResearch	111-035-003	1:5,000	-
Goat anti-Mouse IgG (H+L) Secondary Antibody, Alexa Fluor® 647 conjugate	Thermo fisher scientific	A-21236	-	1:500
Goat anti-Mouse IgG (H+L) Secondary Antibody, Alexa Fluor® 546 conjugate	Thermo fisher scientific	A-11030	-	1:500
Goat anti-Rabbit IgG (H+L) Secondary Antibody, Alexa Fluor® 647 conjugate	Thermo fisher scientific	A-21245	-	1:500
Goat anti-Rabbit IgG (H+L) Secondary Antibody, Alexa Fluor® 546 conjugate	Thermo fisher scientific	A-11035	-	1:500
LysoTracker™ Deep Red	Invitrogen	L12492	-	50 nM

Table S5. Chemicals and Reagents list, Related to Methods

Chemicals and Reagents	Source	Catalog No.
MLN4924 (Pevonedistat)	Active Biochem	A1139
Z-Leu-Leu-Leu-al ≥90% (HPLC) (MG132)	Sigma-Aldrich	C2211
Tubacin	Selleckchem	No.S2239
Chloroquine	Sigma-Aldrich	C6628
Gateway™ LR Clonase™ II Enzyme mix	Invitrogen	11791-100
Lipofectamine™ 2000 Transfection Reagent	Invitrogen	11668
Lipofectamine™ RNAiMAX Transfection Reagent	Invitrogen	13778
Cellfectin® II Reagent	Invitrogen	10362-100
Halt™ Protease Inhibitor Cocktail, EDTA-Free (100X)	Invitrogen	78439
4',6-diamidino-2-phenylindole (DAPI)	Sigma-Aldrich	D9542
Glutathione Sepharose 4B resin	GE Healthcare	17-0756-05
Coomassie Brilliant Blue R-250	Bio-Rad	161-0400
2× Laemmli Sample Buffer	Bio-Rad	161-0737
VECTASHIELD® Antifade Mounting Medium	Vector labs	H-1000
TRIzol™ Reagent	Invitrogen	15596018
SuperSignal™ West Pico Chemiluminescent Substrate	Thermo Scientific	34580
QuikChange Lightning Multi Site-Directed Mutagenesis Kit	Stratagene	210516
High-Capacity cDNA reverse Transcription Kit	Applied Biosystems	4368814
iQ SYBR Green Supermix	Bio-Rad	170-8880

TRANSPARENT METHODS

Plasmids

Entry clones and Gateway destination vectors were purchased from Thermo-Fisher Scientific. All genes present in the entry clones were cloned into appropriate destination vectors using a Gateway LR Cloning system (Invitrogen). Site-directed mutagenesis to generate NEDD8 mutants was performed using a QuikChange site-directed mutagenesis kit (Stratagene). To facilitate protein purification, a pDEST20 destination vector was modified by incorporating DNA sequences corresponding to the human rhinovirus (HRV 3C) cleavage site (3C) or a 3C/V5-tag. All plasmids were validated by DNA sequencing. Detailed information of all constructs and primers used in this study is described in Table S1 and Table S2.

Cell lines and culture

Human osteosarcoma (U2OS) and human cervical cancer (HeLa) cell lines were purchased from the American Type Culture Collection. U2OS and HeLa cells were cultured in Dulbecco's modified Eagle's medium (DMEM) and Minimum Essential Medium (MEM), respectively, supplemented with 10% (v/v) fetal bovine serum (Gibco), 50 units/mL penicillin, and 50 μg/mL streptomycin. Human embryonic kidney (HEK293FT) was purchased from Invitrogen and cultured in DMEM with the same supplements as mentioned above. Cells were maintained at 37 °C with 5% CO_2 in a humidified chamber.

Protein microarray

Protein microarray was generated using a HuProt human proteome microarray v3.0 (CDI Laboratories). The protein chip was equilibrated using microarray buffer (137 mM NaCl; 2.7 mM KCl; 4.3 mM Na_2HPO_4; 1.8 mM KH_2PO_4 pH 7.4; 0.05% Triton X-100) for 5 min at room temperature and then was incubated with 5% skim milk (BD Biosciences), prepared in microarray buffer, for 1 h at room temperature. To screen for NEDD8-binding proteins, a blocked protein chip was washed 3 times with the microarray buffer for 10 min and incubated with 2 μg/mL recombinant GST-NEDD8 in the reaction buffer [50 mM Tris-Cl pH 7.5; 2 mM dithiothreitol (DTT); 2.5 mM $MgCl_2$] for 8 h at 4 °C. Before probing with NEDD8 antibody, the protein chip was washed with the microarray buffer for 10 min. The washed chip was incubated with rabbit

polyclonal NEDD8 antibody (GeneTex, 1:1,000) diluted in microarray buffer containing 1% skim milk for 2 h and was then washed with the microarray buffer 3 times. Then, the chip was incubated with Alexa Fluor goat-anti Rabbit 647-conjugated secondary antibody (1:5,000) for 30 min at room temperature. The chip was washed 3 times with microarray buffer and drained via centrifugation in a 50 mL conical tube (200 *g* for 2 min). Finally, the chip was scanned on a GenePix 4000B instrument (Molecular Devices). GST antibody was used to probe all proteins spotted in chips with Alexa Fluor goat-anti Rabbit 546-conjugated secondary antibody. The signal intensity value for each spot was obtained as the ratio of foreground to background signal and normalized to GST signal intensity. The mean signal intensity of all proteins on the chip was calculated.

Analysis of binding affinity (K_D) between NEDD8 and HDAC6

The NEDD8/GST-HDAC6 binding kinetics were analyzed using bio-layer interferometric measurements and an Octet QKe System (ForteBio). NEDD8 protein (Boston Biochem, 12.5 μM) was loaded onto an Amine Reactive 2nd Gen (AR2G) Biosensor. The association of NEDD8 with 10.4, 20.7, and 41.4 nM GST-HDAC6 was measured over a duration of 300 s. Dissociation was monitored for 1,200 s. K_D value and kinetics were calculated using ForteBio.

Immunofluorescence microscopy

HeLa cells were transfected with *si*RNA and recombinant plasmids using Lipofectamine RNAiMAX (Invitrogen) and Lipofectamine 2000 (Invitrogen), respectively. To induce ubiquitin stress, cells were treated with 5 μM MG132, 3 μM MLN4924, or a combination of MG/MLN. Cells treated with DMSO were used as the negative control. For immunostaining experiments, cells were seeded on glass bottom dishes (SPL). Briefly, cells were fixed using 4% paraformaldehyde prepared in phosphate-buffered saline (PBS, pH 7.4) for 15 min at room temperature and washed three times with PBS. Subsequently, cells were permeabilized with 0.25% Triton X-100 prepared in PBS for 15 min at room temperature and blocked with 1% bovine serum albumin (BSA) prepared in PBS for 30 min at room temperature. Cells were incubated with the indicated primary antibodies for 18 h at 4 °C. Then, the cells were washed and incubated with the Alexa Fluor-conjugated secondary antibody (1:500) for 1 h at room temperature. After washing, the nuclei were stained with 4',6-diamidino-2-phenylindole (Sigma-Aldrich, 1 μg/ml) for 10 min. Finally, cells were mounted onto 1.2 mm glass slides using Vectashield mounting medium (Vector

Labs). Detailed information of all antibodies and chemicals used in this study is described in Table S4 and Table S5.

Purification of recombinant proteins from Sf9 cells

Gateway vectors pDEST20, pDEST20-3C, and pDEST20-3C/V5 were used to generate vectors for the expression of GST-fusion proteins in the Bac-to-Bac Baculovirus Expression System (Invitrogen). To generate recombinant NEDD8, NEDD8 mutants, or HDAC6, pDEST20 expression vectors containing each gene were transformed into DH10Bac *E. coli* (Gibco) to generate recombinant bacmid DNA. Sf9 cells were transfected with purified bacmid DNA (5 μg) using Cellfectin II Reagent (Gibco, 8 μg). Protein expression was evaluated by immunoblotting with anti-GST antibody. Baculoviruses expressing the proteins of interest were cultured twice in T-25 flasks (SPL) to obtain an optimal viral titer. For protein expression, Sf9 cells were transduced with baculovirus stocks, and were collected 3 days after transduction. To purify the GST-fusion proteins, the collected Sf9 cells were lysed using NETN buffer [25 mM Tris-HCl pH 8.0; 150 mM NaCl; 1 mM ethylenediaminetetraacetic acid (EDTA); 1 mM DTT; 1% NP-40; 0.1% Triton X-100; protease inhibitor cocktail; 1 mM phenylmethylsulfonyl fluoride (PMSF)]. The lysate was subjected to centrifugation at 14,000 rpm for 10 min at 4 °C; the supernatant was collected and incubated with Glutathione Sepharose 4B resin (GE Healthcare). The GST-fusion protein—bound resin was washed with NETN buffer and the fusion proteins were eluted using the elution buffer (50 mM 4-(2-hydroxyethyl)-1-piperazineethanesulfonic acid pH 7.5; 40 mM reduced glutathione; 100 mM NaCl; 30% glycerol). The purity of the eluates was confirmed by electrophoresis on 8–16% SDS-PAGE followed by: (1) Coomassie brilliant blue (Bio-Rad) staining and (2) immunoblotting with anti-GST antibody. The protein concentrations were determined using the Bradford method (Bio-Rad). To cleave the GST tag from the purified GST-fusion proteins, each protein was incubated with HRV 3C protease (GE Healthcare) in cleavage buffer (50 mM Tris-HCl pH 7.4; 150 mM NaCl; 1 mM EDTA; 1 mM DTT) for 24 h at 4 °C. The cleaved protein was purified by passing through a GST affinity column that has an affinity for the HRV 3C protease and the GST tag. The purity of the final product was examined by Coomassie brilliant blue staining following electrophoresis on an 8–16% gradient SDS-PAGE. Detailed information of all proteins used in this study is described in Table S3.

Dot-blot assay

For dot-blot analysis, 10 μM (in a final volume of 10 μL) bait protein was placed on a nitrocellulose membrane. Next, the membrane was blocked with 5% skim milk prepared in PBST (PBS containing 0.05% Tween 20) for 30 min at room temperature. The membrane was incubated for 1 h at room temperature with the indicated proteins. After washing with PBST, the membrane was probed with the indicated primary antibody. The membrane was then washed with PBST and incubated with horseradish peroxidase-conjugated secondary antibody (1:5,000) for 1 h at room temperature. After three washes with PBST, the membrane was developed using an ECL kit (Thermo-Fisher Scientific). GST was used as the negative control.

Preparation of whole cell lysates

To prepare whole cell lysates, three different cell lysis methods were used. To check the interaction between HDAC6 and NEDD8 in the immunoprecipitation assay (IP), cells were lysed in lysis buffer as described in the section of Immunoprecipitation. For the immunoblotting assay using whole cell lysates, cells were directly lysed in Laemmli sample buffer (Bio-Rad) supplemented with 8 M Urea. Alternatively, cells were lysed in immunoprecipitation buffer (IPB) (10 mM Tris-HCl pH 7.5; 150 mM NaCl; 5 mM EDTA; 1% NP-40; 0.5% sodium deoxycholate; 1 mM PMSF; protease inhibitor cocktail) to isolate MG/MLN induced-NEDDylated proteins. Briefly, cell lysates were fractionated into supernatants and pellets by centrifugation at 12,000 *g* for 10 min at 4 °C. The first supernatants (S1) were stored on ice and the pellets were dissolved in modified IPB buffer containing 0.1 % SDS. To obtain insoluble NEDDylated proteins, sonication was carried out for 1 minute at 30% output with 5 seconds pulsing and then the last supernatant (S2) was extracted by centrifugation at 12,000 *g* for 10 min at 4 °C. Supernatants including S1 and S2 were combined and then subjected to an immunoprecipitation assay. For the immunoprecipitation of MG/MLN-induced NEDDylated proteins, combined supernatants were incubated with anti-NEDD8 antibody for 12 h at 4 °C. Next, the supernatants were incubated with protein G beads for 12 h at 4 °C and washed with IPB buffer. For the deNEDDylation assay, each sample was incubated with 75 nM His_6-NEDP1 (Boston Biochem) or 20 nM His_6-CYLD (Boston Biochem) in deNEDDylation buffer for 1 h. The reaction was terminated by adding 2× Laemmli sample buffer. NEDDylated proteins were detected by immunoblotting with an anti-NEDD8 or -ubiquitin antibody.

In vitro deNEDDylation assay

HeLa cells were treated with 5 μM MG132, 3 μM MLN4924, or a combination of MG/MLN as described above. Then, cells were lysed using the IPB buffer and then whole cell extracts were prepared by centrifugation at 12,000 *g* for 10 min at 4 °C. For the deNEDDylation assay, each extract was incubated with BSA, 75 nM His_6-NEDP1 or 20 nM His_6-CYLD in the deNEDDylation buffer for various time periods (15 min, 30 min, 1 h at 37 °C or overnight at 4 °C). To avoid non-specific enzymatic activity of NEDP1, *in vitro* deNEDDylation assay was conducted for shorter time durations of 15 min or 1 h. The reaction was terminated by adding 2× Laemmli sample buffer. NEDDylated substrates were detected by immunoblotting with an anti-NEDD8 antibody. BSA was used as the negative control. Purified NEDDylated proteins were also used for deNEDDylation assay as described above. Isolation method of NEDDylated proteins is described in the previous section (See section of Preparation of whole cell lysates).

Immunoprecipitation

HEK293FT cells were transfected with the indicated expression vectors using Lipofectamine 2000 (Invitrogen). After 24 h, the cells were lysed using lysis buffer (0.5% Triton X-100, 0.5% NP-40, 1 mM PMSF, and protease inhibitor cocktail in PBS) and centrifuged at 12,000 *g* for 10 min at 4 °C. For the immunoprecipitation of FLAG-NEDD8, the supernatant was incubated with anti-FLAG M2 affinity gel (Sigma Aldrich) overnight at 4 °C. The beads were washed 4 times with IP buffer and denatured in 2× Laemmli sample buffer (Bio-Rad).

GST pull-down assay

For expression and purification of recombinant GST-p62 protein, full length p62 gene present in the entry clone was sub-cloned into a pDEST20-3C/V5 vector using the Gateway LR Cloning system (Invitrogen). Recombinant GST-p62 protein was purified from insect cells as described above. GST-bead–bound GST-p62 (1 μg) was incubated with cell extracts—of cells in which ubiquitin stress had been induced—in a total reaction volume of 200 μL at 4 °C for 12 h. The beads were then washed four times with lysis buffer and denatured in 2× Laemmli sample buffer. Samples were electrophoresed on 8–16% gradient SDS-PAGE, followed by immunoblotting with the indicated antibodies.

RT-qPCR

siRNAs were transfected into HeLa cells using Lipofectamine RNAiMAX (Invitrogen). Total RNA was extracted from the cells using TRIzol (Invitrogen). cDNA was synthesized using a High Capacity cDNA Reverse Transcription kit (Applied Biosystems). RT-qPCR was performed as previously described (Stefano Amatori, 2017) using iQ SYBR Green Supermix (Bio-Rad) and analyzed using the CFX Manager Software (Bio-Rad). Primer for RT-qPCR was used as following:

UBA1 FP: 5'-CCATAAACGCCTTCATTGGG-3',

UBA1 RP: 5'-TGGAGGCACTTGTCCTCTGTG-3',

GAPDH FP: 5'-GGAGTCAACGGATTTGGTCGTA-3',

GAPDH RP: 5'-GGCAACAATATCCACTTTACCA-3'.

Quantification of ALB-containing cells

All samples were subjected to imaging using a Nikon A1R confocal microscope equipped with a 60× 1.4 NA oil immersion objective at the same experimental setting. For the quantitation of ALB-containing cells, only those with an aggregate size larger than 5 μm^2 were classified as ALB-containing cells, and ALB-containing cells were counted using NIS-Elements AR software (Nikon). For the statistical analysis, cells were counted from 50 to 300.

Statistical analysis

Statistical testing was performed using the GraphPad Prism 6 software. One-way or two-way analysis of variance was used followed by Bonferroni's multiple comparisons tests for analysis of the data. The results are represented a mean ± standard error of mean. $P \leq 0.05$ was considered to be statistically significant. For quantitative analysis of protein expression by immunoblotting, signal intensity of the bands was measured and analyzed using ImageJ.

REFERENCE

Stefano Amatori, G.P., Mirco Fanelli (2017). Real-time quantitative PCR array to study drug-induced changes of gene expression in tumor cell lines. Journal of Cancer Metastasis and Treatment *3*, 90-99.